Principles of Motor Adaptation when Walking with a Powered Exoskeleton

by

Pei-Chun Kao

A dissertation submitted in partial fulfillment
of the requirements for the degree of
Doctor of Philosophy
(Kinesiology)
in The University of Michigan
2009

Doctoral Committee:

Associate Professor Daniel P. Ferris, Chair
Associate Professor Bernard J. Martin
Assistant Professor Riann M. Palmieri-Smith
Assistant Professor Scott G. Mclean
Research Fellow Cara L. Lewis

This dissertation is dedicated to my parents, my older brother and sister, who have always encouraged and supported me

Acknowledgements

This dissertation could not have been accomplished without the support I received from many individuals. First and foremost, I would like to thank my advisor, Dan Ferris. I am lucky to have Dan as my advisor because Dan always provides great assistance and mentor in many aspects during my graduate studies. Especially, the way of how Dan approaches research questions I learnt from him will save me tremendous time in trial and error during my future careers.

I would like to thank my committee members, Bernard Martin, Riann Smith, Scott Mclean and Cara Lewis for providing critical suggestions to my study designs to make the projects more complete. In particular, I would like to thank Riann for the initial development of the H-reflex testing and the help of trouble-shooting on different stimulators. Cara has been a great colleague to work with and provided me a lot of assistance. If Cara didn't come up with the brilliant real-time program in testing H-reflex response, there would be no chapter 4 in my dissertation and I might have graduated at least 6 months earlier (?).

All current and previous members of Human Neuromechanics Laboratory have provided me assistance in collecting data and feedbacks in writing articles. I would like to especially thank Danielle Sandella and Evelyn Anaka for meticulous data collections, Kristin Carroll for tremendous data tracking, and Anne Manier

for fabricating the orthoses. I also would like to thank my human subjects for patience and tolerance to the long testing protocols and the unpleasant electrical stimulations. I also would like to acknowledge the funding sources, NIH R21 to Dan Ferris and Kinesiology teaching fellowship.

The work in this dissertation was supported by NIH R21 NS062119.

Chapters 2 and 3 of this dissertation are published and currently in review, respectively. Chapters 4 and 5 have been prepared for publication in Neuroscience Letters and the Journal of Physiology, respectively.

Kao PC, and Ferris DP. Motor adaptation during dorsiflexion-assisted walking with a powered orthosis. Gait and Posture 29: 230-236, 2009.

Kao PC, Lewis CL, and Ferris DP. Invariant ankle moment patterns when walking with and without a robotic ankle exoskeleton. Journal of Biomechanics. In review, 2009.

Kao PC, Lewis CL, and Ferris DP. Short-term locomotor adaptation to a robotic ankle exoskeleton does not alter soleus Hoffmann reflex amplitude. To be submitted, 2009.

Kao PC, Lewis CL, and Ferris DP. Joint kinetic response during unexpectedly reduced plantar flexor torque provided by a robotic ankle exoskeleton during walking. To be submitted, 2009.

Table of Contents

List of Figures

Figure

Abstract

Robotic exoskeletons are currently developed to augment human motor performance or assist in the gait rehabilitation of individuals with neurological injuries. While the robotic technology is rapidly advancing, there is a large gap in our understanding of how humans respond to exoskeleton assistance during locomotion. To build successful robotic devices, it is critical to understand the principles governing mechanical human-machine interaction. In this dissertation, I used lightweight ankle exoskeletons powered by artificial pneumatic muscles to provide mechanical assistance to neurologically intact human subjects. The exoskeletons allowed me to investigate some general principles of motor adaptation in human walking. In the first experiment, an exoskeleton provided subjects with increased dorsiflexor torque. The results demonstrated that there are different adaptation responses for the type bursts of tibialis anterior recruitment during walking. In the second experiment, an exoskeleton provided plantar flexor torque with two artificial pneumatic muscles, increasing the exoskeleton mechanical output compared to past studies. With this assistance, subjects rapidly decreased soleus recruitment to walk with a total ankle moment pattern similar to unassisted gait. However, subjects adapted at a slower rate for the stronger exoskeleton. In the third experiment, I quantified soleus monosynaptic reflex responses to determine if reflex inhibition is one of the

mechanisms for reducing soleus recruitment during robotic-assisted walking. Subjects demonstrated similar soleus H-reflex amplitudes corresponding to background muscle activation during powered versus unpowered walking. This indicates the reflex gain is not modified during short-term adaptation to the robotic exoskeleton. In the final experiment, I used the exoskeleton as a tool to quantify the mechanical output of plantar flexor reflex responses during perturbed gait. I introduced a perturbation by turning off the robotic assistance unexpectedly in midstance. During the perturbed steps, subjects greatly increased muscle activation to maintain total ankle moment patterns similar to unperturbed steps. Overall these studies demonstrated that the nervous system prioritizes a given ankle joint moment pattern during human walking, both with robotic assistance and when encountering gait perturbations. The combined results of these experiments will help guide the design of future robotic devices and could lead to better strategies for robotic-assisted gait rehabilitation.

Chapter I

Introduction

Many research groups are developing robotic exoskeletons which aim to assist motor rehabilitation for individuals after neurological injuries. As a rehabilitation tool, the primary goals of robotic exoskeletons are to reduce manual assistance from therapists and to achieve optimal training outcomes. Although the first objective has been realized by many current robotic devices, producing better rehabilitation outcomes with robotic devices is still a developing area of research. To design better robotic devices, it is important to understand the principles governing how humans learn to interact with the robotic assistance and to identify the gait parameters humans prioritize as objectives for their gait pattern.

I used two types of robotic exoskeletons to examine rapid locomotor adaptation to mechanical assistance. The specific questions I addressed were: (1) how do neurologically intact subjects adapt their walking patterns to a powered orthosis that provides dorsiflexion assistance? (2) Do subjects walk with joint kinetic patterns during robotic-assisted walking similar to joint kinetic patterns during unassisted walking? (3) Is locomotor adaptation rate dependent on exoskeleton strength? (4) Is an increased stretch reflex inhibition a potential

mechanism for reducing soleus recruitment when walking with the exoskeleton? (5) Do stretch reflex responses during unexpected gait perturbations appropriately meet the mechanical requirements of gait?

In the first experiment, the exoskeleton was configured to provide dorsiflexion assistance proportional to the voluntary activation of the tibialis anterior muscle (i.e., ankle dorsiflexor). For the rest of experiments, the exoskeleton was configured with two artificial pneumatic muscles providing plantar flexion assistance proportional to the soleus muscle activation (i.e., ankle plantar flexor). The double muscle exoskeleton provided twice the mechanical capability of the previous single-muscle exoskeleton design (Cain et al. 2007; Gordon and Ferris 2007; Kinnaird and Ferris 2009). The results provide important insights into the principles governing human locomotor adaptation. The information can be used to aid in designing powered devices and may be helpful in optimizing gait rehabilitation therapies. In addition, the findings should be helpful in the development of biologically realistic neuromusculoskeletal computer simulations of human walking.

Background

Neurologically impaired individuals usually demonstrate gait deficits caused by insufficient muscle strength and discoordination (Nadeau et al. 1999; Chen et al. 2005b; Bohannon 2007; Den Otter et al. 2007; Lamontagne et al. 2007; Patterson et al. 2007; Turns et al. 2007; Chen and Patten 2008; Scivoletto et al. 2008). For example, their slow walking speed is associated with a marked

reduction in ankle push-off at late stance. In addition, individuals after neurological injuries (such as stroke, spinal cord injury, cerebral palsy, traumatic brain injury) usually demonstrate hyper-active reflex responses that substantially affect their movement capabilities (Lamontagne et al. 2001; Dietz 2002; Lamontagne et al. 2007). The inability to modulate their soleus stretch reflex response during walking may worsen their gait patterns (Sinkjaer et al. 1995; Trimble et al. 1998) and decrease efficiency further (Waters and Mulroy 1999). Thus, inefficient and unstable gait patterns would discourage them from walking and indirectly lead to a general deconditioning.

Task specific locomotor training can greatly improve walking ability in people after neurological injuries as independent walking is one of the primary goals in locomotion rehabilitation. Treadmill training with body weight support (BWSTT) with or without manual assistance (Chen et al. 2005a; Moseley et al. 2005; Peurala et al. 2005; Dobkin et al. 2006), or with functional electrical stimulation (Field-Fote 2001), has shown promising therapeutic effects on walking ability (e.g. gait patterns, speeds, and functional levels) for people after neurological injuries (Hesse et al. 1995; Visintin et al. 1998; Wernig et al. 1998; Sullivan et al. 2002). This gait therapy usually requires two to three therapists to assist the leg stepping motion and to stabilize the trunk. During training, therapists tend to provide assistance that helps patients achieve nearly normal kinematics. Repetitions of normal walking kinematics and spatiotemporal pattern provided during BWSTT may also aid in normalizing reflex modulation (Phadke et al. 2007).

Due to the labor-intensive nature of BWSTT, robotic devices are developed for assisting in locomotion training. The advantages of robotic devices are to enable a more intensive training protocol (i.e. as much training as needed) and to reduce manual assistance needed from therapists. The Mechanized Gait Trainer (MGT) (Hesse et al. 1999; Hesse et al. 2000; Werner et al. 2002), Lokomat (Colombo et al. 2001; Wirz et al. 2005), ARTHuR (Ambulation-assisting Robotic Tool for Human Rehabilitation), PAM (Pelvic Assist Manipulator) and POGO (Penumatically Operated Gait Orthosis) (Reinkensmeyer et al. 2006; Aoyagi et al. 2007) are examples of current robotic devices that incorporate BWSTT. Although these robotic gait trainers greatly reduce the demand of manual assistance, the nature of automation in stepping assistance may promote the patients to become passive. Passivity would lead to a reduction in activity-dependent plasticity. In addition, few devices have been tested that can assist at the ankle. The latter point is important in that a reduced ankle push-off at late stance has been shown to be a major factor limiting walking capabilities in people after neurological injuries (Nadeau et al. 1999; Chen et al. 2005b; Lamontagne et al. 2007; Chen and Patten 2008) and lack of ankle dorsiflexion during swing may cause a substantial stability issue for the patients. However, there is no general agreement on control methods for robotic assistance that can achieve better rehabilitation outcomes than traditional therapy.

To design better robotic gait devices that can enhance the therapy, it is critical to investigate fundamental mechanisms governing the locomotor adaptation to the robotic assistance as well as what parameters are prioritized by

the nervous system for achieving steady state walking dynamics. However, there are only a handful of studies that have quantified the human motor response to powered lower limb exoskeletons compared to the number of different exoskeletons being developed around the world. This is a hurdle to future exoskeleton development that needs to be overcome (Dollar and Herr 2008).

Due to the abnormally high spasticity seen in the neurologically impaired individuals, it has been believed that training protocols or devices that can aid in normalizing abnormal reflexes may accelerate gait rehabilitation. Studies on body-weight supported treadmill training and skillful cycling have shown that performance improvements are associated with decreased soleus H-reflex amplitudes both in healthy subjects (Mazzocchio et al. 2006) and people with spinal cord injuries (Trimble et al. 1998; Trimble et al. 2001; Phadke et al. 2007). Recalibration of reflex responses may be one of the neural mechanisms involved in the motor adaptation during robotic-assisted walking. The changes in joint mechanics during robotic-assisted walking are likely to affect the excitability of multiple sensory feedback loops, many of which contribute to muscle recruitment during walking. However, no study has examined the reflex responses during robotic-assisted versus unassisted walking.

Being able to predict gait dynamic parameters that remain fairly invariant with and without robotic assistance would greatly aid in robotic exoskeleton design for healthy, neurologically intact subjects. This would allow engineers to reliably estimate the mechanical output of the exoskeleton during different tasks. One possible parameter of gait that could be used to predict the exoskeleton

behavior is the kinematic pattern. Some studies have suggested that people control their kinematic patterns to maintain the covariance of limb segment elevation angles (i.e. the angle between the segment and the vertical) (Bianchi et al. 1998a; Bianchi et al. 1998b; Lacquaniti et al. 1999; Lacquaniti et al. 2002). The kinematic relationship has been shown to be robust both in forward and backward locomotion and its nature is not altered by perturbing gait patterns and changing gait speed (Lacquaniti et al. 1999). In addition, kinematic patterns may be a good predictor of mechanical energy expenditure according to a significant correlation between kinematics (i.e. the phase shift of inter-segmental covariance on the elevation angles) and the net mechanical power output. As a result, the kinematic tuning strategy may be used by the nervous system during robotic-assisted walking.

Another possible parameter of gait dynamics that could be used to predict the exoskeleton behavior is the overall support moment during stance. Winter has demonstrated a fairly consistent pattern of support moment (i.e. sum of extensor moments across hip, knee and ankle joints) during stance phase in human walking (Winter 1980) across different speeds (Winter 1989). Joint moment at the knee and hip are highly variable but their sum is less variable. In addition, ankle joint moment is least variable and very consistent at different walking speeds (Winter 1983). More generally, it seems that kinetic parameters have better predictability across walking speeds than kinematic parameters (Lelas et al. 2003; Shemmell et al. 2007). Dynamic moments generated from hip, knee and ankle have been found to be tightly coupled during the swing phase of

gait as well (Shemmell et al. 2007). The findings from these studies support the idea that joint moments may be intrinsically represented in the neural control of human walking and that they have an important mechanical consequence on the gait dynamics (Winter and Eng 1995; Prilutsky et al. 2005). However, it is still unknown what parameters are prioritized by the nervous system during robotic-assisted walking.

An issue related to robotic exoskeletons is how to minimize the time period of motor adaptation required to smoothly use exoskeleton assistance. Is it better to turn on the power all at once, or is it better to slowly increase the power? It has been suggested that augmenting movement errors may improve motor learning for the robotic assisted reaching (Patton et al. 2006) and walking tasks (Emken and Reinkensmeyer 2005; Reinkensmeyer et al. 2006; Emken et al. 2007). However, introducing too much robotic power at once may not necessarily speed up the adaptation process. Subjects might increase their joint impedance when encountering excessive robotic assistance that greatly perturbs the movement dynamics.

In this dissertation, I have addressed some of these major questions regarding how humans adapt to robotic exoskeleton assistance during walking. The results provide insights into the primary principles governing locomotor adaptation may help guide design of future robotic devices, could lead to new ways that exoskeletons can aid gait rehabilitation, and should be useful in developing physiologically realistic neuromusculoskeletal computer simulations of human walking.

References

Aoyagi D, Ichinose WE, Harkema SJ, Reinkensmeyer DJ, Bobrow JE (2007) A robot and control algorithm that can synchronously assist in naturalistic motion during body-weight-supported gait training following neurologic injury. IEEE Transactions on Neural Systems and Rehabilitation Engineering 15: 387-400

Bianchi L, Angelini D, Lacquaniti F (1998a) Individual characteristics of human walking mechanics. Pflugers Archives - European Journal of Physiology 436: 343-356

Bianchi L, Angelini D, Orani GP, Lacquaniti F (1998b) Kinematic coordination in human gait: relation to mechanical energy cost. Journal of Neurophysiology 79: 2155-2170.

Bohannon RW (2007) Muscle strength and muscle training after stroke. Journal of Rehabilitation Medicine 39: 14-20

Cain SM, Gordon KE, Ferris DP (2007) Locomotor adaptation to a powered ankle-foot orthosis depends on control method. Journal of Neuroengineering and Rehabilitation 4

Chen G, Patten C (2008) Joint moment work during the stance-to-swing transition in hemiparetic subjects. Journal of Biomechanics 41: 877-883

Chen G, Patten C, Kothari DH, Zajac FE (2005a) Gait deviations associated with post-stroke hemiparesis: improvement during treadmill walking using weight support, speed, support stiffness, and handrail hold. Gait & Posture 22: 57-62

Chen G, Patten C, Kothari DH, Zajac FE (2005b) Gait differences between individuals with post-stroke hemiparesis and non-disabled controls at matched speeds. Gait & Posture 22: 51-56

Colombo G, Wirz M, Dietz V (2001) Driven gait orthosis for improvement of locomotor training in paraplegic patients. Spinal Cord 39: 252-255

Den Otter AR, Geurts ACH, Mulder T, Duysens J (2007) Abnormalities in the temporal patterning of lower extremity muscle activity in hemiparetic gait. Gait & Posture 25: 342-352

Dietz V (2002) Proprioception and locomotor disorders. Nature Reviews Neuroscience 3: 781-790

Dobkin B, Apple D, Barbeau H, Basso M, Behrman A, Deforge D, Ditunno J, Dudley G, Elashoff R, Fugate L, Harkema S, Saulino M, Scott M, Grp S (2006) Weight-supported treadmill vs overground training for walking after acute incomplete SCI. Neurology 66: 484-492

Dollar AM, Herr H (2008) Lower extremity exoskeletons and active orthoses: Challenges and state-of-the-art. Ieee Transactions on Robotics 24: 144-158

Emken JL, Benitez R, Sideris A, Bobrow JE, Reinkensmeyer DJ (2007) Motor adaptation as a greedy optimization of error and effort. Journal of Neurophysiology 97: 3997-4006

Emken JL, Reinkensmeyer DJ (2005) Robot-enhanced motor learning: accelerating internal model formation during locomotion by transient

dynamic amplification. IEEE Transactions on Neural Systems and Rehabilitation Engineering 13: 33-39
Field-Fote EC (2001) Combined use of body weight support, functional electric stimulation, and treadmill training to improve walking ability in individuals with chronic incomplete spinal cord injury. Archives of Physical Medicine and Rehabilitation 82: 818-824
Gordon KE, Ferris DP (2007) Learning to walk with a robotic ankle exoskeleton. Journal of Biomechanics 40: 2636-2644
Hesse S, Bertelt C, Jahnke MT, Schaffrin A, Baake P, Malezic M, Mauritz KH (1995) Treadmill training with partial body weight support compared with physiotherapy in nonambulatory hemiparetic patients. Stroke 26: 976-981
Hesse S, Uhlenbrock D, Sarkodie-Gyan T (1999) Gait pattern of severely disabled hemiparetic subjects on a new controlled gait trainer as compared to assisted treadmill walking with partial body weight support. Clinical Rehabilitation 13: 401-410
Hesse S, Uhlenbrock D, Werner C, Bardeleben A (2000) A mechanized gait trainer for restoring gait in nonambulatory subjects. Archives of Physical Medicine and Rehabilitation 81: 1158-1161
Kinnaird CR, Ferris DP (2009) Medial gastrocnemius myoelectric control of a robotic ankle exoskeleton for human walking. IEEE Transactions on Neural Systems and Rehabilitation Engineering 17: 31-37
Lacquaniti F, Grasso R, Zago M (1999) Motor patterns in walking. News in Physiological Sciences 14: 168-174
Lacquaniti F, Ivanenko YP, Zago M (2002) Kinematic control of walking. Arch Ital Biol 140: 263-272
Lamontagne A, Malouin F, Richards CL (2001) Locomotor-specific measure of spasticity of plantarflexor muscles after stroke. Archives of Physical Medicine and Rehabilitation 82: 1696-1704
Lamontagne A, Stephenson JL, Fung J (2007) Physiological evaluation of gait disturbances post stroke. Clinical Neurophysiology 118: 717-729
Lelas JL, Merriman GJ, Riley PO, Kerrigan DC (2003) Predicting peak kinematic and kinetic parameters from gait speed. Gait & Posture 17: 106-112
Mazzocchio R, Kitago T, Liuzzi G, Wolpaw JR, Cohen LG (2006) Plastic changes in the human H-reflex pathway at rest following skillful cycling training. Clinical Neurophysiology 117: 1682-1691
Moseley AM, Stark A, Cameron ID, Pollock A (2005) Treadmill training and body weight support for walking after stroke. Cochrane Database of Systematic Reviews
Nadeau S, Gravel D, Arsenault AB, Bourbonnais D (1999) Plantarflexor weakness as a limiting factor of gait speed in stroke subjects and the compensating role of hip flexors. Clinical Biomechanics 14: 125-135
Patterson SL, Forrester LW, Rodgers MM, Ryan AS, Ivey FM, Sorkin JD, Macko RF (2007) Determinants of walking function after stroke: Differences by deficit severity. Archives of Physical Medicine and Rehabilitation 88: 115-119

Patton JL, Stoykov ME, Kovic M, Mussa-Ivaldi FA (2006) Evaluation of robotic training forces that either enhance or reduce error in chronic hemiparetic stroke survivors. Experimental Brain Research 168: 368-383

Peurala SH, Tarkka IM, Pitkanen K, Sivenius J (2005) The effectiveness of body weight-supported gait training and floor walking in patients with chronic stroke. Archives of Physical Medicine and Rehabilitation 86: 1557-1564

Phadke CP, Wu SS, Thompson FJ, Behrman AL (2007) Comparison of soleus H-reflex modulation after incomplete spinal cord injury in 2 walking environments: Treadmill with body weight support and overground. Archives Of Physical Medicine And Rehabilitation 88: 1606-1613

Prilutsky BI, Sirota MG, Gregor RJ, Beloozerova IN (2005) Quantification of motor cortex activity and full-body biomechanics during unconstrained locomotion. Journal of Neurophysiology 94: 2959-2969

Reinkensmeyer DJ, Aoyagi D, Emken JL, Galvez JA, Ichinose W, Kerdanyan G, Maneekobkunwong S, Minakata K, Nessler JA, Weber R, Roy RR, de Leon R, Bobrow JE, Harkema SJ, Edgerton VR (2006) Tools for understanding and optimizing robotic gait training. Journal of Rehabilitation Research and Development 43: 657-670

Scivoletto G, Romanelli A, Mariotti A, Marinucci D, Tamburella F, Mammone A, Cosentino E, Sterzi S, Molinari M (2008) Clinical factors that affect walking level and performance in chronic spinal cord lesion patients. Spine 33: 259-264

Shemmell J, Johansson J, Portra V, Gottlieb GL, Thomas JS, Corcos DM (2007) Control of interjoint coordination during the swing phase of normal gait at different speeds. Journal of Neuroengineering and Rehabilitation 4

Sinkjaer T, Toft E, Hansen HJ (1995) H-reflex modulation during gait in multiple sclerosis patients with spasticity. Acta Neurol Scand 91: 239-246

Sullivan KJ, Knowlton BJ, Dobkin BH (2002) Step training with body weight support: effect of treadmill speed and practice paradigms on poststroke locomotor recovery. Archives of Physical Medicine and Rehabilitation 83: 683-691

Trimble MH, Behrman AL, Flynn SM, Thigpen MT, Thompson FJ (2001) Acute effects of locomotor training on overground walking speed and H-reflex modulation in individuals with incomplete spinal cord injury. Journal of Spinal Cord Medicine 24: 74-80

Trimble MH, Kukulka CG, Behrman AL (1998) The effect of treadmill gait training on low-frequency depression of the soleus H-reflex: comparison of a spinal cord injured man to normal subjects. Neuroscience Letters 246: 186-188

Turns LJ, Neptune RR, Kautz SA (2007) Relationships between muscle activity and anteroposterior ground reaction forces in hemiparetic walking. Archives of Physical Medicine and Rehabilitation 88: 1127-1135

Visintin M, Barbeau H, Korner-Bitensky N, Mayo NE (1998) A new approach to retrain gait in stroke patients through body weight support and treadmill stimulation. Stroke 29: 1122-1128.

Waters RL, Mulroy S (1999) The energy expenditure of normal and pathologic gait. Gait & Posture 9: 207-231

Werner C, Von Frankenberg S, Treig T, Konrad M, Hesse S (2002) Treadmill training with partial body weight support and an electromechanical gait trainer for restoration of gait in subacute stroke patients: a randomized crossover study. Stroke 33: 2895-2901

Wernig A, Nanassy A, Muller S (1998) Maintenance of locomotor abilities following Laufband (treadmill) therapy in para- and tetraplegic persons: follow-up studies. Spinal Cord 36: 744-749

Winter DA (1980) Overall principle of lower limb support during stance phase of gait. Journal of Biomechanics 13: 923-927

Winter DA (1983) Biomechanical motor patterns in normal walking. Journal of Motor Behavior 15: 302-330

Winter DA (1989) BIOMECHANICS OF NORMAL AND PATHOLOGICAL GAIT - IMPLICATIONS FOR UNDERSTANDING HUMAN LOCOMOTOR CONTROL. Journal of Motor Behavior 21: 337-355

Winter DA, Eng P (1995) Kinetics: our window into the goals and strategies of the central nervous system. Behavioural Brain Research 67: 111-120

Wirz M, Zemon DH, Rupp R, Scheel A, Colombo G, Dietz V, Hornby TG (2005) Effectiveness of automated locomotor training in patients with chronic incomplete spinal cord injury: A multicenter trial. Archives of Physical Medicine and Rehabilitation 86: 672-680

Chapter II

Motor adaptation during dorsiflexion-assisted walking with a powered orthosis

Abstract

A robotic ankle-foot orthosis (AFO) that provides powered assistance could adjust to varying gait dynamics much better than a rigid AFO. To provide insight into how humans would adapt to a powered AFO, we studied the response of neurologically intact subjects walking with an active dorsiflexion assist orthosis proportionally controlled by tibialis anterior electromyography (EMG). We examined the two mechanical functions of ankle dorsiflexors in gait (power absorption at heel strike and power generation at toe-off) by recruiting two groups of healthy subjects: Group One, called Continuous Control, (n=5) had dorsiflexion assistance both at the initial heel contact and during swing; Group Two, called Swing Control, (n=5) had the assistance only during swing. We hypothesized both groups of subjects would reduce tibialis anterior EMG amplitude with practice walking with the powered dorsiflexion assist. Ten healthy subjects were fitted with custom-made orthoses that included an artificial pneumatic muscle providing dorsiflexor torque. We collected lower body kinematics, EMG, and artificial muscle force while subjects walked on a treadmill

for two 30-minute training sessions. We found that subjects walked with increased ankle dorsiflexion by 9 degrees but showed different adaptation responses of the two tibialis anterior EMG bursts. The first EMG burst around heel strike had ~28% lower amplitudes (p<0.05) but the second EMG burst during swing had similar amplitudes. These results provide baseline data of EMG controlled dorsiflexion assist in neurologically intact humans that can be used to guide future studies on neurologically impaired individuals.

Key words: Gait; Locomotion; Powered orthosis; Electromyography; Rehabilitation

Introduction

Rigid ankle-foot orthoses (AFO) are frequently prescribed for patients with very weak dorsiflexor recruitment to improve walking ability and prevent tripping. However, drawbacks to rigid AFOs are that they impede active plantar flexion at push-off and do not allow users to make step-to-step changes in motion dynamics (e.g. altering speed, adapting to surface terrain, etc). Many research groups are developing powered orthoses or robotic exoskeletons to help people with gait deficits (Blaya and Herr 2004; Ferris et al. 2005; Ferris et al. 2006) or to augment human performance (Kawamoto and Sankai 2002; Lee and Sankai 2005; Kazerooni and Steger 2006). The orthoses could be used as everyday gait aids to improve mobility or as rehabilitation tools to shape the motor patterns of patients (Ferris et al. 2005). A critical aspect dictating the success of robotic

orthoses for either purpose is how people react to the active devices. Understanding the human response should make it easier to design powered orthoses that achieve either of the goals.

The purpose of this study was to examine how healthy, neurologically intact humans adapt their walking patterns to a powered orthosis that provides dorsiflexion assistance. The advantage of a powered AFO with dorsiflexion assist is that it would not impede plantar flexion at the end of stance and would allow users to make alterations in their gait to accommodate changes in the environment. We used proportional myoelectric control of the powered orthosis because our prior research has shown that humans can quickly adapt to plantar flexion assistance with proportional myoelectric control (Gordon and Ferris 2007). The current study allowed us to examine the same type of motor adaptation test for the dorsiflexors.

The tibialis anterior has two main bursts of activity during gait: one at heel strike to slowly lower the foot to the ground and one at toe-off to help provide toe clearance during swing. The former provides mechanical power absorption at the ankle joint and the latter provides mechanical power generation at the ankle joint. To examine these different mechanical functions, we recruited two groups of healthy subjects: (1) one group of subjects received active dorsiflexion assistance both at heel strike and during swing – Continuous Control; (2) another group of subjects received assistance only during swing – Swing Control. Assistance provided at all phases of the gait cycle (Continuous Control) is easiest from an engineering perspective because ongoing EMG signals

throughout the gait cycle can be used to control timing and amplitude of the assistance. However, our previous studies using artificial pneumatic muscles to power robotic lower limb orthoses have suggested that the human nervous system tends to avoid activating the orthoses for power absorption (Sawicki and Ferris 2006; Gordon and Ferris 2007). As a result, we also wanted to test a control mode that would rely on the orthosis only for power generation. The swing control group allowed us to test if assistance given only during power generation phase (i.e. stance-to-swing transition) resulted in different motor adaptation than assistance during both phases.

We hypothesized that both groups would reduce tibialis anterior EMG amplitude and return to normal joint kinematics with practice walking with the powered dorsiflexion assist. Gordon and Ferris (Gordon and Ferris 2007) found that healthy subjects walking with a powered orthosis providing plantar flexion assistance under proportional myoelectric control of soleus reduced soleus EMG by ~35% to walk with nearly normal joint kinematics in just two 30-minute sessions. We generated our hypothesis and study protocol based on these prior results studying human locomotor adaptation to a powered orthosis (Gordon and Ferris 2007).

Methods

Subjects

Ten healthy subjects (five male, five female, age: 18-31 years) gave written informed consent and participated in the study. The University of Michigan Medical School Institutional Review Board approved the protocol.

Experimental design

We constructed a custom-made orthosis (Fig. 1) for left lower limb of each subject. The orthosis consisted of polypropylene shank and foot sections. An artificial pneumatic muscle attached on the two portions powers the orthosis for providing augmented dorsiflexor torque. We implemented proportional myoelectric control (i.e., amplitude and timing) of the artificial muscle through a desktop computer and real-time control board (dSPACE Inc.). A custom software program regulated air pressure in the artificial muscle proportional to the processed tibialis anterior EMG. EMG signal from tibialis anterior was high-pass filtered with a second-order Butterworth filter (20-Hz cutoff frequency) to remove movement artifact, full wave rectified, and low-pass filtered with a second-order Butterworth filter (10-Hz cutoff frequency) to smooth the signal. Adjustable gains scaled the control signals and a threshold cutoff eliminated background noise. In Continuous Control, control signals came from the processed tibialis anterior EMG signals throughout the gait cycle. In Swing Control, the right-side footswitch was used for gating control signals.

Subjects completed two identical testing sessions 72 hours apart. During each session, subjects walked with the orthosis first without power for 10 minutes (baseline), with power for 30 minutes (active), and without power again for 15 minutes (post-adaptation). Before testing, subjects were not given any practice

walking with the orthosis. We chose this testing protocol to match a similar study from our laboratory testing the effects of powered plantar flexion assistance using soleus proportional myoelectric control (Gordon and Ferris 2007).

Data acquisition and analysis

We recorded lower body kinematics, artificial muscle force, and electromyography during the first 10 seconds (~7 full strides) of every minute while subjects walked on a treadmill at 1.25 m/s. The three-dimensional kinematic data were collected by using 8-camera video system (120 Hz, Motion Analysis Corporation, Santa Rosa, CA). Artificial muscle force data were collected with a force transducer (1200 Hz, Omega Engineering). We placed bipolar surface electrodes on the left lower limb to record EMGs (1200 Hz, Konigsberg Instruments Inc.) from tibialis anterior (TA), soleus (SOL), medial gastrocnemius (MG), lateral gastrocnemius (LG), vastus lateralis (VL), vastus medialis (VM), rectus femoris (RF) and medial hamstring muscles (MH). Electrode position was marked on subjects using permanent ink to assure consistent placement.

All data were time normalized to 100% of stride cycle (i.e., from left heel strike to its next one). To quantify changes in muscle activation, we calculated root-mean-square (RMS) amplitude of the high-pass filtered (20-Hz cutoff frequency) and rectified EMG for each burst of tibialis anterior individually. For the first burst, we calculated sum of the RMS over 90-100% and 0-10% of gait cycle. For the second burst, we calculated RMS over 50-90% of gait cycle. For all

ther muscles, we calculated RMS over whole gait cycle. We normalized them to the last minute of baseline on a given testing session.

The joint angles were calculated from smoothed marker data (4^{th} order Butterworth zero-lag low-pass filter, 6-Hz cutoff frequency). To examine changes in kinematics across time for ankle, knee and hip joint angles, we linearly correlated the average joint angle profile during the powered condition at each minute to the average joint angle profile at the last minute of baseline on a given testing session using Pearson product moment correlation. As 10 seconds of data were recorded each minute, the correlations reflected the average of about 7 strides of data. The common variance (r^2) of the correlation was used as a quantitative measure of similarity in joint kinematics. This method has been quantitatively assessed for validity by Derrick et al (1994) (Derrick et al. 1994).

There are many ways to quantify motor adaptation when studying human movement. A common approach is to use exponential or power law fits of a behavioral parameter. The main drawback to this approach is that mounting literature has established that there are at least two independent processes with different time scales underlying motor adaptation (Smith et al. 2006). As a result, quantifying an adaptation rate from an exponential or power fit is inherently flawed. We chose to use a measure of performance variability to quantify adaptation rate (Noble and Prentice 2006). For data with a normal distribution, approximately 95% of all values should lie within the mean ± two standard deviations. Based on this rule of probability, we have defined steady state performance using the mean ± two standard deviations of data from the last 15

minutes on the second day of testing. The slope of a linear regression fit to the last 15 data points on Day 2 was not significantly different from zero (t-test, $p>0.05$). Using time to steady state as the measure of motor adaptation rate does not make any a priori assumptions about the shape of the motor adaptation data or the number of processes with different time scales involved in the motor adaptation. The method is described in more detail in Noble and Prentice (Noble and Prentice 2006) and Gordon and Ferris (Gordon and Ferris 2007). We calculated time to steady state for the tibialis anterior RMS EMG and the ankle angle correlation.

To estimate the amount of assistance provided (e.g. percent of normal dorsiflexor torque during walking) by the powered orthosis, we calculated net ankle joint torque and power from ten trials of over-ground walking at 1.25 m/s without wearing orthosis. We used commercial software (Visual3D, C-Motion Inc.) to perform inverse dynamic calculations. Lower limb inertial properties were estimated based on anthropometric measurements of subjects (Zatsiorsky 2002).

Statistical analysis

We used repeated measure factorial ANOVAs (2-way) to test for differences in normalized EMG RMS (primary outcome variables were the two bursts of tibialis anterior EMG), joint angle correlation common variances (primary outcome variable was for the ankle joint) between days and conditions (baseline, powered walking minute 1, 15 and 30) (2 days x 4 conditions). Thus, we had three primary outcome variables. We analyzed other parameters as secondary outcome variables to provide insight into the overall adaptation.

Included in the secondary outcome variables were the differences in adaptation periods of the two bursts of tibialis anterior EMG RMS and the ankle joint angle correlation common variance between days and groups. We used additional repeated measure factorial ANOVAs (2 days x 2 groups) for the adaptation periods. We set the significance level at $p<0.05$ and used Tukey Honestly Significant Difference (THSD) post hoc tests for pair-wise comparisons if a main effect was detected.

Results

Joint Kinematics

Subjects walked with substantially increased ankle dorsiflexion when the assistance was provided (Fig. 2). Continuous Control subjects increased ankle dorsiflexion both at initial heel contact and during swing by ~9 degrees. Continuous Control subjects also increased knee flexion (by ~8 degrees) during initial stance along with the increased dorsiflexion to walk in a slightly more crouched posture. Swing Control subjects also increased ankle dorsiflexion during swing by ~9 degrees.

Although both groups of subjects showed some adaptation over the 30-minute session, there were still large differences in ankle joint kinematics between steady state assistance at the end of Day 2 and baseline. For both groups, the ankle angle correlation common variance (r^2) at the first minute was the lowest during all testing (Fig. 3). Continuous Control subjects had reduced plantar flexion at push-off during initial powered walking but returned to nearly

normal plantar flexion by the end of Day 2. Correspondingly, ankle angle correlation common variance was higher at minute 30 compared to minute 1 for Continuous Control (Fig. 3). However, throughout active trials of both days, ankle angle correlation common variance of Continuous Control subjects was significantly different from baseline (ANOVA, $p<0.001$, Power=1.00) due to augmented dorsiflexion at initial stance and mid- to late-swing. Swing Control subjects increased ankle dorsiflexion during mid- to late-swing without reducing plantar flexion at push-off. Swing Control ankle angle correlation common variance throughout active trials was also significantly different from baseline (ANOVA, $p<0.001$, Power=1.00) due to consistent augmented dorsiflexion.

There were no large differences in knee or hip joint angle profiles for either group with one exception. Continuous Control had greater knee flexion (~8 degrees) during initial stance ($p=0.098$). Knee and hip joint angle correlation common variances were always greater than 0.96 for all powered trials. There were no significant differences (THSD, $p>0.05$) between active and baseline conditions in the knee (day 2, minute 30: Continuous Control 0.97±0.02, Swing Control 0.98±0.03, mean±SD) or hip (day 2, minute 30: Continuous Control 0.99±0.01, Swing Control 0.99±0.01) joint angle correlation common variance (r^2) for either group after 30-min training.

Orthosis Mechanics

The powered orthosis provided greater peak ankle dorsiflexor torques (Fig. 4) than those normally occurring during walking. At the end of Day 2, the orthosis provided peak dorsiflexor torques of 0.22±0.14 Nm/kg (mean±SD) for

Continuous Control subjects around initial heel contact, and 0.12±0.09 Nm/kg for Continuous Control and 0.11±0.06 Nm/kg for Swing Control subjects during swing. The normal peak dorsiflexor torque during over-ground walking for the ten subjects was 0.17±0.07 Nm/kg at heel strike and 0.02±0.00 Nm/kg at swing (mean±SD).

Electromyography (EMG)

During active trials, the shape of the tibialis anterior EMG patterns was similar to baseline trials (Fig. 5) but there were fluctuations in EMG amplitudes. For minute 1 on Day 1, Continuous Control subjects had significantly lower tibialis anterior EMG amplitudes for the first but not the second burst. The Continuous Control reduction in the first burst became more marked on the second day (ANOVA, $p<0.001$, Power=0.97) (Fig. 5). Compared to baseline, the first tibialis anterior EMG burst had ~28% lower amplitudes at the end of powered walking (day 2, minute 30: 0.72±0.15, mean±SD, THSD, $p<0.05$). The second tibialis anterior EMG burst was similar in amplitude at the end of the second day (0.86±0.17, THSD, $p>0.05$). In Swing Control subjects, there was a similar response for the second tibialis anterior EMG burst. On Day 2, the second tibialis anterior EMG burst amplitude was similar to baseline for Swing Control (1.08±0.08 for minute 1 and 1.15±0.28 for minute 30, THSD, $p>0.05$).

There were some increases in EMG amplitudes for other lower limb muscles during initial activation but the EMG amplitudes at the end of Day 2 were similar to baseline values. In Continuous Control, soleus, medial gastrocnemius, lateral gastrocnemius, rectus femoris, and medial hamstrings demonstrated

increased activation during the initial powered walking. In Swing Control, there were no substantial changes in other lower limb EMG amplitudes. By the end of Day 2, both groups had similar shapes of muscle activation patterns to baseline during powered walking.

Adaptation Rates

Both groups of subjects reached steady state in both kinematics and tibialis anterior EMG amplitude within the two-day training but demonstrated faster adaptation on Day 2 than on Day 1. For ankle angle correlation common variance, both groups reached steady state more rapidly in the second session (ANOVA, $p<0.001$, Power=1.00) (mean±SD: Day One 28.6±3.1 min, Day Two 6.4±5.5 min for Continuous Control; Day One 29.6±0.9 min, Day Two 11.8±6.3 min for Swing Control) but there was no significant difference between the two groups in time to steady state (THSD, $p>0.05$) on both days. For tibialis anterior EMG amplitudes, both groups reached steady state more rapidly on Day 2 than Day 1 for both bursts (ANOVA, $p=0.001$, Power=0.96). For the first tibialis anterior EMG burst, Swing Control subjects reached steady state faster than Continuous Control subjects on Day 1 (THSD, $p<0.05$) (Day One 25.0±4.7 min, Day Two 8.8±5.1 min for Continuous Control; Day One 12.6±13.6 min, Day Two 0.6±0.9 min for Swing Control) but there was no significant difference in adaptation rates for the second EMG burst (THSD, $p>0.05$) (Day One 23.8±9.1 min, Day Two 5.2±4.9 min for Continuous Control; Day One 18.6±15.6 min, Day Two 3.4±4.7 min for Swing Control).

Discussion

The powered orthosis provided substantial ankle dorsiflexor torque at the target phases. The ankle kinematics, torque and power data (Fig. 2, 4) indicated that the powered orthosis reduced plantar flexion at initial heel contact and augmented dorsiflexion during swing phase. Development of a portable dorsiflexion assist orthosis that provides similar torques as the one tested in this study may help people with weak ankle dorsiflexors to reduce foot slap at heel strike and improve foot clearance during swing.

Using proportional myoelectric control in post-stroke patients presents both problems and opportunities. For patients with appropriate timing but weak amplitudes, a dorsiflexion assist orthosis with proportional myoelectric control could provide increased ankle motion under direct control by the nervous system. For patients with disordered timing of tibialis anterior, they are likely to have inappropriate initial patterns in orthosis assistance. However, the patients may also demonstrate adaptation in their recruitment patterns as healthy subjects did in this study. The added mechanical torque provided by the orthosis may actually enhance motor learning as it would produce greater errors in movement dynamics for inappropriate recruitment patterns. Error is the driving stimulus for motor learning, so greater error from the power of the orthosis could theoretically enhance motor recovery (Emken and Reinkensmeyer 2005; Patton et al. 2006a; Patton et al. 2006b). Future studies need to examine how post-stroke and other neurologically impaired populations respond to practice walking with robotic orthosis under proportional myoelectric control.

The limitation of our current design is that it is not readily portable due to the type of actuator used (i.e. pneumatic artificial muscle). However, the portability could be improved by using a micro-air compressor (Bharadwaj et al. 2005) for pneumatic artificial muscle or to use other types of actuators such as Series Elastic Actuator (SEA) (Pratt et al. 2002; Pratt et al. 2004) instead. One example of current built dorsiflexion assist devices is the active AFO by Blaya and Herr (Blaya and Herr 2004). They used a series elastic actuator to adjust impedance of the orthosis using information from ankle angle sensor and force sensors beneath the foot.

Our findings indicate that subjects had different adaptation responses for ankle dorsiflexors during the two main phases of activation. Subjects walked with substantially increased ankle dorsiflexion without altering tibialis anterior EMG at the second burst during stance-to-swing transition. This similar response of second burst in both groups (i.e. without decreasing amplitude) indicated that assistance given only during power generation phase did not result in different motor adaptation during the concentric phase of tibialis anterior activation. In contrast, tibialis anterior EMG was reduced by ~28% at the first burst during swing-to-stance transition. During this phase, the tibialis anterior is activated eccentrically to perform negative mechanical work as the foot is lowered to the ground. As a result, the findings only partially supported our hypothesis that subjects would reduce tibialis anterior recruitment when walking with a powered dorsiflexion assist proportional to tibialis anterior EMG.

Different adaptation responses of the two tibialis anterior EMG bursts might be explained by analyzing the costs and benefits of adaptation. The added dorsiflexion assistance during stance-to-swing transition may not provide a very strong stimulus for neuromuscular adaptation. There is no penalty in the mechanics of leg swing to have exaggerated ankle dorsiflexion during swing. The foot simply clears a higher height without added cost to the wearer. From the aspect of gait energetics, leg swing consumes ~30% of net energy required for walking (Doke et al. 2005) but hip flexors and plantar flexors are the main muscles responsible (Meinders et al. 1998; Neptune et al. 2001; Siegel et al. 2004; Gottschall and Kram 2005). Ankle dorsiflexion itself consumes a fairly small amount of energy because the foot segment has very low mass. Thus, the energy savings from turning down tibialis anterior activation during the second burst may not be a strong enough stimulus for the nervous system to quickly adapt. In contrast, activation of the tibialis anterior at heel strike helps to smoothly lower the forefoot to the ground. Exaggerated ankle dorsiflexion at heel strike could cause instability because it prevents the foot from contacting the ground. Thus, the user would likely substantially benefit from turning down the first burst of tibialis anterior EMG when dorsiflexion assistance is provided by the orthosis.

The cost-benefit analysis would also explain why subjects using plantar flexion assist rapidly reduced their soleus EMG (Gordon and Ferris 2007). During walking, positive work is required to restore the energy lost in redirecting the center of mass velocity from step to step (Donelan et al. 2002) and majority of

the positive work is provided by the ankle muscles (Neptune et al. 2004; Kuo et al. 2005; Neptune and Sasaki 2005). With such high energy production at the ankle, subjects would likely greatly benefit from having some plantar flexion work replaced by a powered orthosis. In the Gordon and Ferris study (2007) (Gordon and Ferris 2007), subjects indeed reduced their soleus EMG amplitudes by ~30% with powered plantar flexion assistance. Our recent work has shown that this substitution of biological muscle work with robotic muscle work can significantly reduce the metabolic cost of walking (Sawicki and Ferris 2008).

Conclusion

Healthy subjects wearing dorsiflexion assist orthoses under proportional myoelectric control walked with increased dorsiflexion but did show some reduction in muscle recruitment of Tibialis anterior. The nervous system modulated individual bursts of tibialis anterior EMG (heel strike and toe-off) differently in regard to motor adaptation. Future studies could use active dorsiflexion assist controlled by EMG as a potential rehabilitation intervention for individuals with dorsiflexor weakness.

Acknowledgments

This work was supported by NIH R01 NS045486. The authors thank Catherine Kinnaird and members of the Human Neuromechanics Laboratory for assistance in collecting data. We also thank Jake Godak and Anne Manier for their contribution to the design and fabrication of the orthosis.

Figures

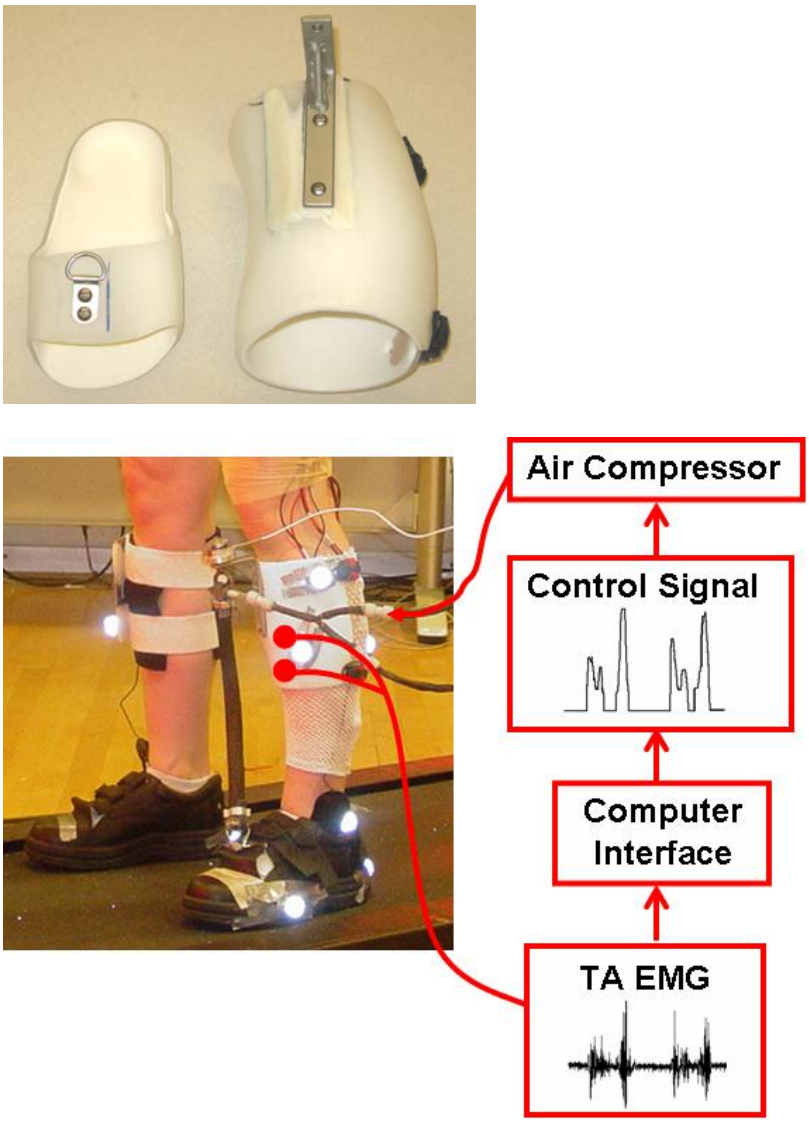

Figure 2.1 Powered orthosis.
Subjects wore a custom fit orthosis on their left lower limb. The orthosis consisted of polypropylene shank and foot sections. The moment arm length (13.9±0.8 cm, mean±SD) and the pneumatic muscle length (38.4±1.8 cm, mean±SD) varied and depended on the feet size and leg length of the subject. Electrical signals (EMG) of tibialis anterior were recorded and processed to be used to control air pressure in the artificial pneumatic muscle proportionally. As air pressure increased, the artificial muscle started to develop tension and shortened, allowing the powered orthosis to provide dorsiflexor torque controlled by tibialis anterior muscle activation.

Figure 2.2 Joint kinematics.
Ankle, knee and hip joint kinematic patterns are shown for the last minute of baseline condition (baseline, red dashed line), the first minute of active condition (minute 1, black line), and the last minute of active condition (minute 30, grey line) on the two training sessions for Continuous Control (n=5) and Swing Control (n=5) subjects. Data are the average of all subjects of each group. The vertical lines represent the toe-off. The ankle joint angle profiles showed greatly increased dorsiflexion by ~9 degrees around the initial heel contact for Continuous Control, and swing phase for both groups on both days. The hip and knee joint angle profiles were similar to the baseline across all testing conditions.

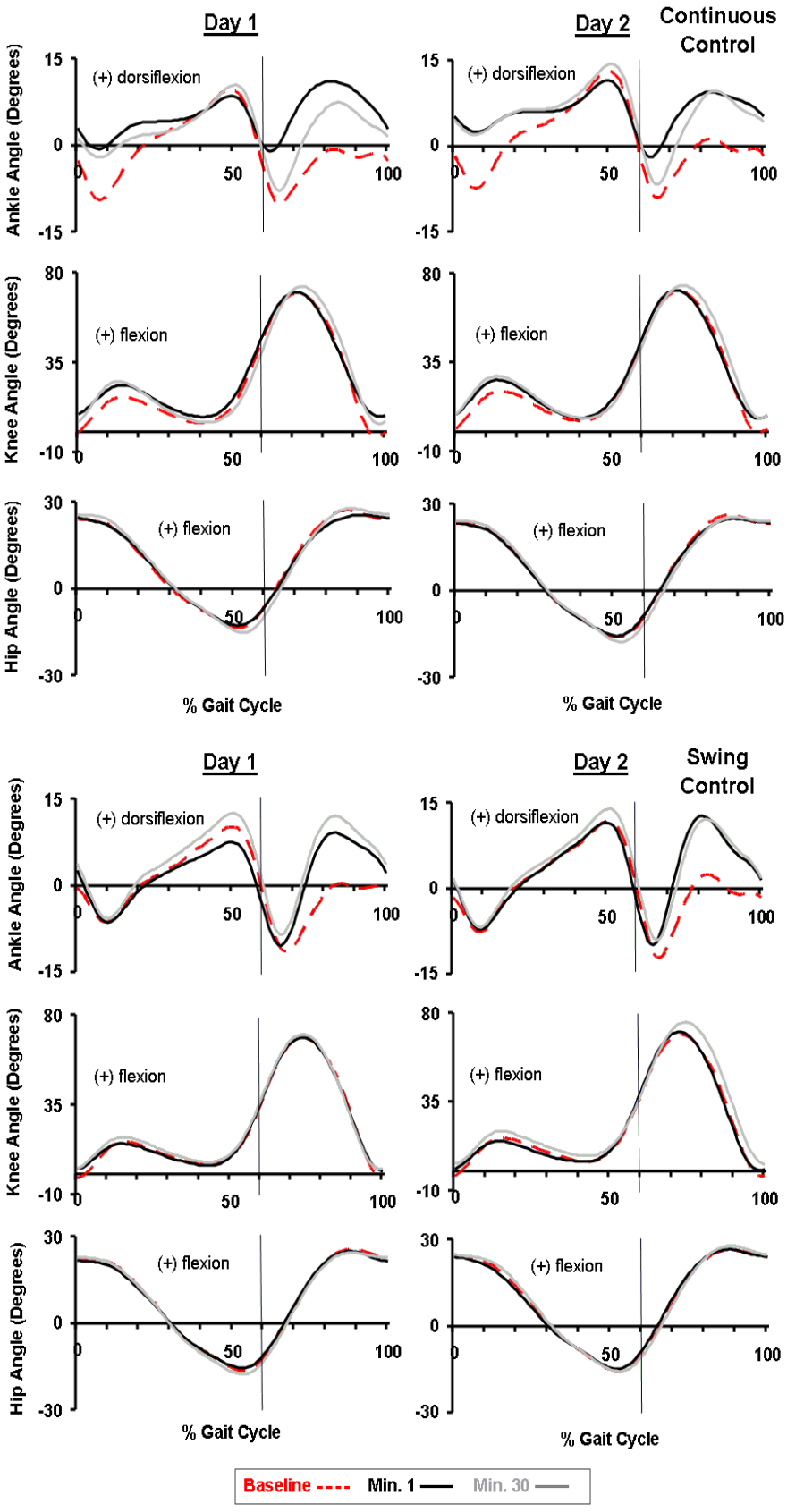
Day 1
Day 2
Continuous Control
Swing Control
Ankle Angle (Degrees)
Knee Angle (Degrees)
Hip Angle (Degrees)
(+) dorsiflexion
(+) flexion
% Gait Cycle
Baseline
Min. 1
Min. 30

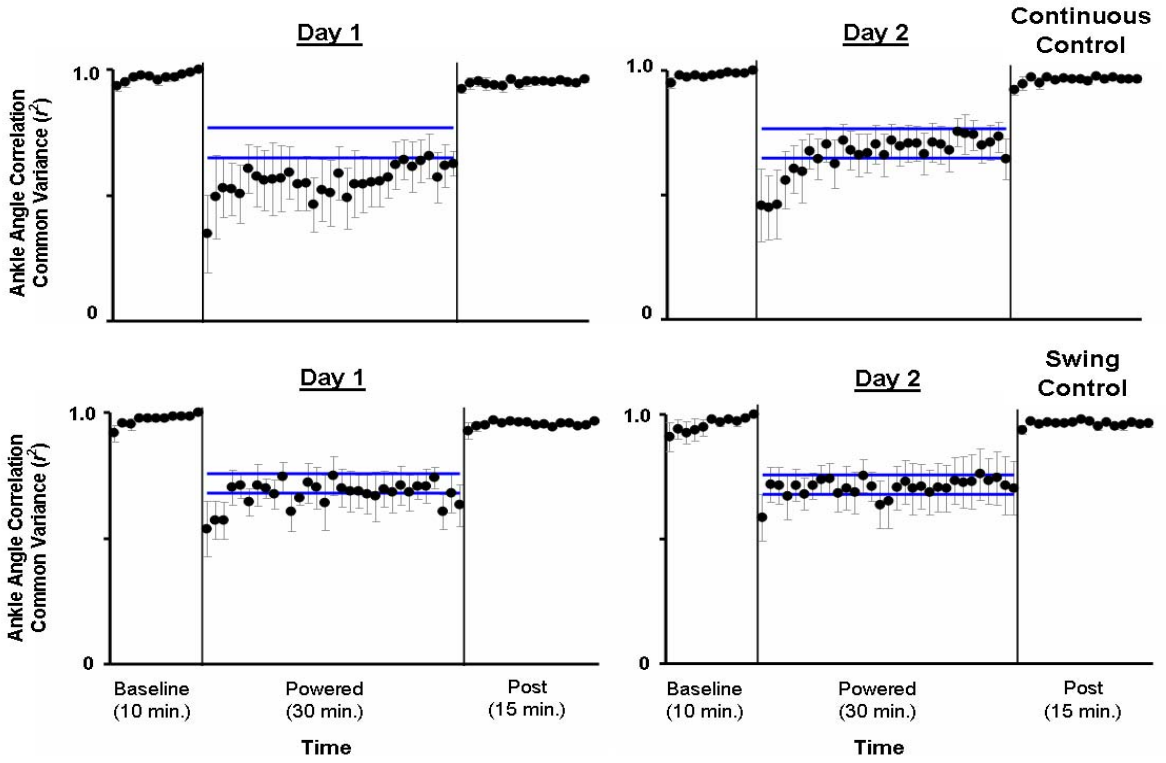

Figure 2.3 Ankle joint angle correlation common variance (r^2).
Mean data (black dots) ± 1 standard error of mean (grey bar) are shown for each minute. The two horizontal blue lines are the mean ± 2 standard deviations from the last 15 minutes of active condition on day 2, representing steady state dynamics. The steady state envelopes shown above from the averaged group data are for display purposes. Steady state dynamics were determined for each subject, individually. Ankle joint angle correlation common variance (r^2) increased with practice in the active condition. However, by the end of active condition on Day 2 (Day 2, minute 30), the values of ankle joint angle correlation common variance in both groups were still significantly different from baseline (mean±SD: Continuous Control: 0.64±0.19, Swing Control: 0.70±0.24, THSD, $p<0.05$).

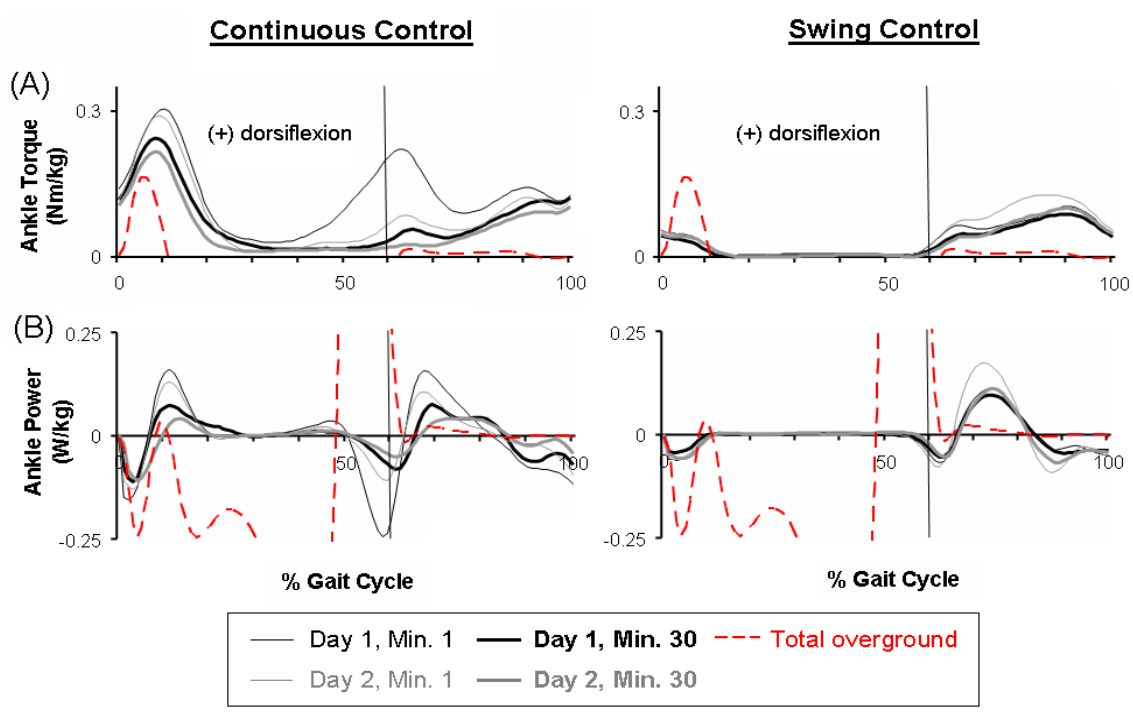

Figure 2.4 Mechanics of the powered orthosis.
(A) Dorsiflexor torque provided by the orthosis. These averaged data (black and grey lines) from all subjects of each group represent only the portion of ankle torque produced by the orthosis (calculated from artificial muscle force and muscle moment arm) during active condition (the first and last minute on both days). Average ankle torque (red dashed line) during overground walking with no orthosis was calculated from inverse dynamics. The overground walking data shown above is zoomed in to the similar range of the powered orthosis data due to relatively small dorsiflexor torque production during normal walking. **(B)** Dorsiflexor power provided by the orthosis. The positive value represents power generation and negative value represents power absorption. These averaged data (black and grey lines) from all subjects of each group represent only the portion of ankle power produced by the orthosis during active condition. Average ankle power (red dashed line) was calculated from inverse dynamics during overground walking with no orthosis.

Figure 2.5 Tibialis anterior activation patterns and tibialis anterior EMG RMS amplitudes of individual bursts.
(A) Tibialis anterior EMG linear envelopes (rectified and low-pass filtered EMG with 6-Hz cutoff frequency) were averaged from all subjects of each group. During initial walking with the powered orthosis (day 1, minute 1, black line), Continuous Control subjects had lower EMG amplitude of the first burst (swing-to-stance transition, period of pink bar) but had greater EMG amplitude of the second burst (stance-to-swing transition, period of light grey bar with oblique lines). By the end of powered walking on the second day (day 2, minute 30, grey line), the amplitude of the first burst remained reduced but the second burst was similar to the baseline (baseline, red dashed line). During initial walking with the powered orthosis (day 1, minute 1), the amplitude of the first burst in Swing Control also reduced but became similar to the baseline after one training session. In addition, the second burst in Swing Control was similar to the baseline. **(B)** EMG RMS amplitudes of the first tibialis anterior burst (90-100% and 0-10% of the gait cycle); and **(C)** EMG RMS amplitudes of the second tibialis anterior burst (50-90% of the gait cycle). Mean data (black dots) ± 1 standard error of mean (grey bar) are shown for each minute. The two horizontal blue lines are the mean ± 2 standard deviations from the last 15 minutes of active condition on day 2, representing steady state dynamics. The steady state envelopes shown above from the averaged group data are for display purposes. Steady state dynamics were determined by each subject, individually.

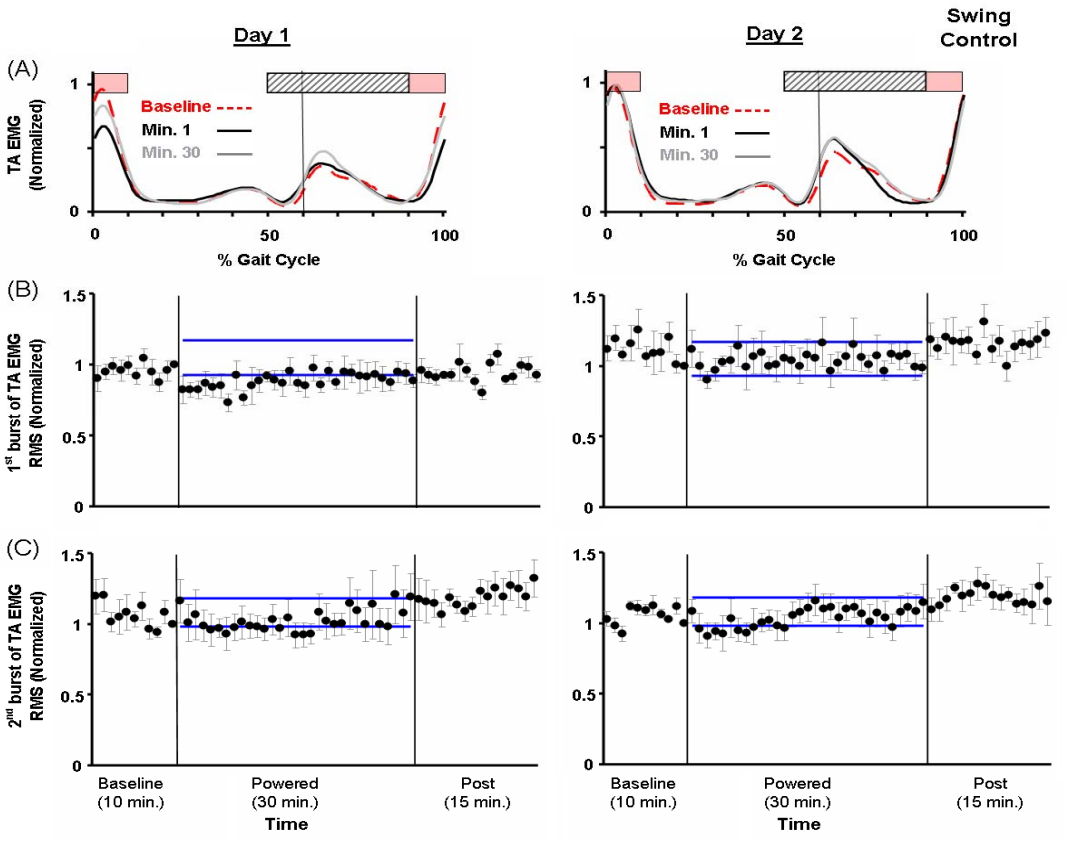
Swing Control
Day 1
Day 2
(A)
TA EMG (Normalized)
Baseline
Min. 1
Min. 30
% Gait Cycle
(B)
1st burst of TA EMG RMS (Normalized)
(C)
2nd burst of TA EMG RMS (Normalized)
Baseline (10 min.)
Powered (30 min.)
Post (15 min.)
Time

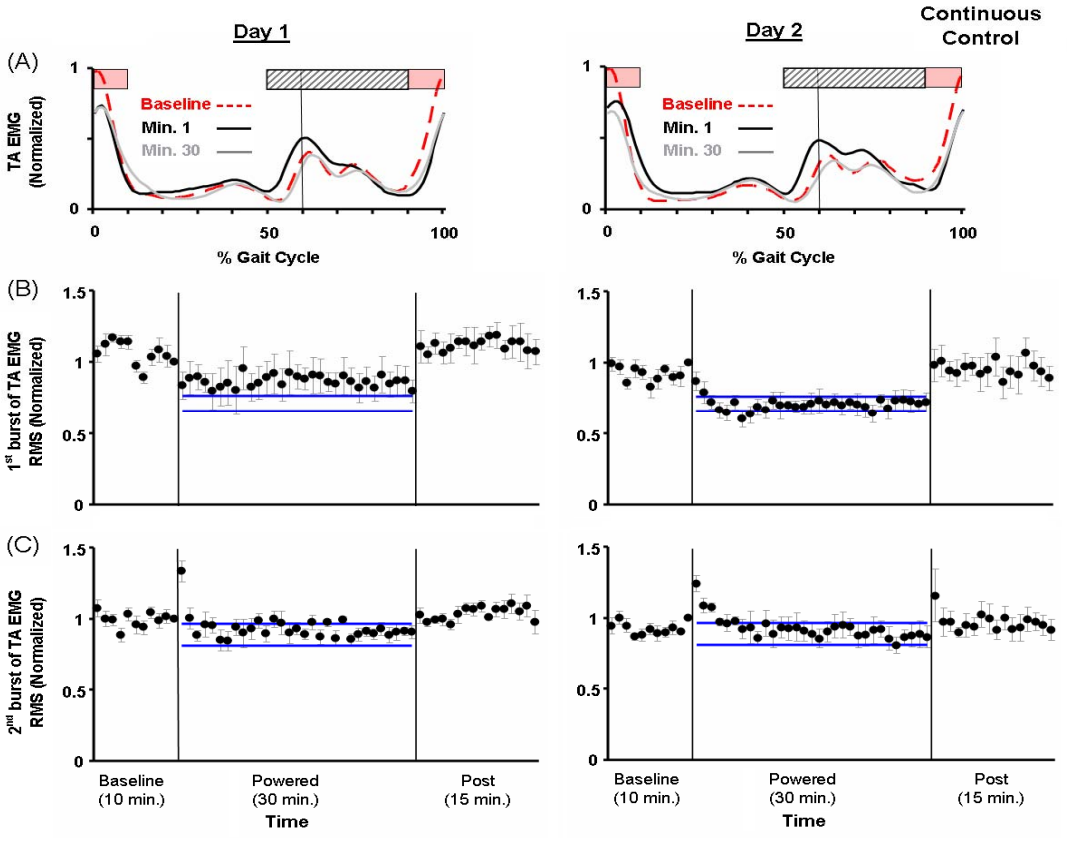
Continuous Control
Day 1
Day 2
(A)
TA EMG (Normalized)
Baseline
Min. 1
Min. 30
% Gait Cycle
(B)
1st burst of TA EMG RMS (Normalized)
(C)
2nd burst of TA EMG RMS (Normalized)
Baseline (10 min.)
Powered (30 min.)
Post (15 min.)
Time

References

Bharadwaj K, Sugar TG, Koeneman JB, Koeneman EJ (2005) Design of a robotic gait trainer using spring over muscle actuators for ankle stroke rehabilitation. Journal of Biomechanical Engineering 127: 1009-1013

Blaya JA, Herr H (2004) Adaptive control of a variable-impedance ankle-foot orthosis to assist drop-foot gait. IEEE Transactions on Neural Systems and Rehabilitation Engineering 12: 24-31

Derrick TR, Bates BT, Dufek JS (1994) Evaluation of Time-Series Data Sets Using the Pearson Product-Moment Correlation-Coefficient. Medicine and Science in Sports and Exercise 26: 919-928

Doke J, Donelan JM, Kuo AD (2005) Mechanics and energetics of swinging the human leg. Journal of Experimental Biology 208: 439-445

Donelan JM, Kram R, Kuo AD (2002) Mechanical work for step-to-step transitions is a major determinant of the metabolic cost of human walking. Journal of Experimental Biology 205: 3717-3727

Emken JL, Reinkensmeyer DJ (2005) Robot-enhanced motor learning: accelerating internal model formation during locomotion by transient dynamic amplification. IEEE Transactions on Neural Systems and Rehabilitation Engineering 13: 33-39

Ferris DP, Gordon KE, Sawicki GS, Peethambaran A (2006) An improved powered ankle-foot orthosis using proportional myoelectric control. Gait and Posture 23: 425-428

Ferris DP, Sawicki GS, Domingo A (2005) Powered lower limb orthoses for gait rehabilitation. Topics in Spinal Cord Injury Rehabilitation 11: 34-49

Gordon KE, Ferris DP (2007) Learning to walk with a robotic ankle exoskeleton. Journal of Biomechanics 40: 2636-2644

Gottschall JS, Kram R (2005) Energy cost and muscular activity required for leg swing during walking. Journal of Applied Physiology 99: 23-30

Kawamoto H, Sankai Y (2002) Comfortable power assist control method for walking aid by HAL-3. In: IEEE International Conference on Systems, Man and Cybernetics, vol 4, pp 1-6

Kazerooni H, Steger R (2006) The Berkeley Lower Extremity Exoskeleton. Journal of Dynamic Systems Measurement and Control-Transactions of the ASME 128: 14-25

Kuo AD, Donelan JM, Ruina A (2005) Energetic consequences of walking like an inverted pendulum: step-to-step transitions. Exercise and Sport Sciences Reviews 33: 88-97

Lee S, Sankai Y (2005) Virtual impedance adjustment in unconstrained motion for an exoskeletal robot assisting the lower limb. Advanced Robotics 19: 773-795

Meinders M, Gitter A, Czerniecki JM (1998) The role of ankle plantar flexor muscle work during walking. Scandinavian Journal of Rehabilitation Medicine 30: 39-46

Neptune RR, Kautz SA, Zajac FE (2001) Contributions of the individual ankle plantar flexors to support, forward progression and swing initiation during walking. Journal of Biomechanics 34: 1387-1398

Neptune RR, Sasaki K (2005) Ankle plantar flexor force production is an important determinant of the preferred walk-to-run transition speed. Journla of Experimental Biology 208: 799-808

Neptune RR, Zajac FE, Kautz SA (2004) Muscle mechanical work requirements during normal walking: the energetic cost of raising the body's center-of-mass is significant. Journal of Biomechanics 37: 817-825

Noble JW, Prentice SD (2006) Adaptation to unilateral change in lower limb mechanical properties during human walking. Experimental Brain Research 169: 482-495

Patton JL, Kovic M, Mussa-Ivaldi FA (2006a) Custom-designed haptic training for restoring reaching ability to individuals with poststroke hemiparesis. Journal of Rehabilitation Research and Development 43: 643-656

Patton JL, Stoykov ME, Kovic M, Mussa-Ivaldi FA (2006b) Evaluation of robotic training forces that either enhance or reduce error in chronic hemiparetic stroke survivors. Experimental Brain Research 168: 368-383

Pratt J, Krupp B, Morse C (2002) Series elastic actuators for high fidelity force control. Industrial Robot 29: 234-241

Pratt JE, Krupp BT, Morse CJ, Collins SH (2004) The RoboKnee: an exoskeleton for enhancing strength and endurance during walking. In: IEEE International Conference on Robotics and Automation. IEEE Press, New Orleans, LA, pp 2430-2435

Sawicki GS, Ferris DP (2006) Mechanics and control of a knee-ankle-foot orthosis (KAFO) powered with artificial pneumatic muscles. In: Proceedings of the 5th World Congress of Biomechanics, July 29 - August 4, Munich, Germany

Sawicki GS, Ferris DP (2008) Mechanics and energetics of level walking with powered ankle exoskeletons. Journal of Experimental Biology 211: 1402-1413

Siegel KL, Kepple TM, Stanhope SJ (2004) Joint moment control of mechanical energy flow during normal gait. Gait Posture 19: 69-75

Smith MA, Ghazizadeh A, Shadmehr R (2006) Interacting adaptive processes with different timescales underlie short-term motor learning. PLoS Biol 4: e179

Zatsiorsky VM (2002) Kinetics of Human Motion. Human Kinetics, Champaign, IL

Chapter III

Invariant ankle moment patterns when walking with and without a robotic ankle exoskeleton

Abstract

To guide development of robotic lower limb exoskeletons, it is necessary to understand how humans adapt to powered assistance. The purposes of this study were to quantify joint moments while healthy subjects adapted to a robotic ankle exoskeleton and to determine if the period of motor adaptation is dependent on the magnitude of robotic assistance. The pneumatically-powered ankle exoskeleton provided plantar flexor torque controlled by the wearer's soleus electromyography (EMG). Eleven naïve individuals completed two 30-min sessions walking on a split-belt instrumented treadmill at 1.25 m/s while wearing the ankle exoskeleton. After two sessions of practice, subjects reduced their soleus EMG activation by ~36% and walked with total ankle moment patterns similar to their unassisted gait (r^2 = 0.98±0.02, THSD, p>0.05). They had substantially different ankle kinematic patterns compared to their unassisted gait (r^2 = 0.79±0.12, THSD, p<0.05). Not all of the subjects reached a steady state gait pattern within the two sessions, in contrast to a previous study using a weaker robotic ankle exoskeleton (Gordon and Ferris 2007). Our results strongly

suggest that humans aim for similar joint moment patterns when walking with robotic assistance rather than similar kinematic patterns. In addition, greater robotic assistance provided during initial use results in a longer adaptation process than lesser robotic assistance.

Key words: Gait; powered orthosis; locomotion; inverse dynamics; joint kinetics; EMG

Introduction

Robotic lower limb exoskeletons hold considerable potential to improve human mobility, serve as gait rehabilitation tools, and study the physiology of human locomotion (Ferris et al. 2005b; Ferris et al. 2007). In order to guide robotic exoskeleton development, it is critical to identify principles of human motor adaptation and to discover the parameters that affect the rate of motor adaptation to the powered assistance. However, there are only a handful of studies that have quantified the human motor response to powered lower limb exoskeletons compared to the number of different exoskeletons being developed around the world. This is a hurdle to future exoskeleton development that needs to be overcome (Dollar and Herr 2008).

Being able to predict some gait dynamic parameters that remain fairly invariant with and without exoskeleton assistance would greatly aid in robotic exoskeleton design. This would allow engineers to reliably estimate the mechanical output of the exoskeleton during different tasks. One possible

parameter of gait dynamics that could be used for predicting exoskeleton behavior is the overall support moment during stance. Winter (Winter 1980; Winter 1989) demonstrated a consistent pattern across a range of speeds when summing extensor moments from the hip, knee and ankle joints during stance in human walking. More generally, it seems that kinetic parameters have better predictability across walking speeds than kinematic parameters (Lelas et al. 2003; Shemmell et al. 2007). Dynamic torques generated from hip, knee and ankle have been found to be tightly coupled during the swing phase of gait as well (Shemmell et al. 2007). The findings from these studies support the idea that joint moments may be intrinsically represented in the neural control of human walking and that they have an important mechanical consequence on the gait dynamics (Winter and Eng 1995; Prilutsky et al. 2005).

In a recent study from our laboratory, we examined how healthy young subjects adjusted to a robotic ankle exoskeleton under proportional myoelectric control (Gordon and Ferris 2007). When the exoskeleton mechanical assistance was first introduced, subjects walked on the ball of their foot due to the increased plantar flexion torque. By the end of two thirty-minute training sessions, subjects had substantially reduced soleus electromyography (EMG) amplitude by ~35% and reached steady state walking dynamics (Gordon and Ferris 2007). That study found that subjects had adopted kinematic patterns with exoskeleton assistance that were similar to kinematic patterns without assistance but did not measure joint kinetics via inverse dynamics.

Another important issue related to robotic exoskeletons is the period of motor adaptation required to smoothly use the exoskeleton assistance. In our previous study (Gordon and Ferris 2007), we measured changes in electromyographic, kinematic, and kinetic parameters during training to determine how much walking practice was required to reach steady state dynamics. Interestingly, we found that using gastrocnemius EMG for control instead of soleus EMG (Kinnaird and Ferris 2009), or using a kinematic based controller instead of proportional myoelectric control (Cain et al. 2007) did not result in different times to reaching steady state in naïve users of the robotic ankle exoskeletons. Thus, it may be that the mechanical capabilities of the robotic exoskeleton are what determine how long it takes to adapt to the robotic assistance.

The purposes of this study were to determine if human subjects walking with a robotic ankle exoskeleton: (1) had similar joint moment profiles during powered versus unpowered walking; and (2) if greater mechanical assistance affected the rate of motor adaptation. We used a robotic ankle exoskeleton similar to that used in previous studies (Cain et al. 2007; Gordon and Ferris 2007; Sawicki and Ferris 2008; Kinnaird and Ferris 2009; Sawicki and Ferris 2009a; Sawicki and Ferris 2009b) but with two artificial pneumatic muscles in parallel providing plantar flexor torque in response to the wearer's soleus muscle activity. Subjects walked on a force-measuring treadmill (Collins et al. 2009) during two training sessions so we could calculate joint kinetics. We hypothesized that subjects would walk with similar joint moment patterns for

powered versus unpowered exoskeleton gait. We also hypothesized that subjects would take a longer time period to reach steady state dynamics with the double-muscle robotic ankle exoskeleton compared to the single-muscle exoskeleton (Gordon and Ferris 2007) due to the greater mechanical perturbation.

Methods

Subjects

11 healthy subjects (6 female, 5 male) gave written informed consent and participated in the study. The University of Michigan Medical School Institutional Review Board approved the protocol.

Experimental design

We constructed a custom-made exoskeleton (Fig 1) for the left lower limb of each subject. Details of the design and performance of the exoskeleton are documented elsewhere (Ferris et al. 2005a; Ferris et al. 2006; Gordon et al. 2006). We implemented proportional myoelectric control (i.e., amplitude and timing) of the artificial muscles through a desktop computer and real-time control board (dSPACE Inc.). A custom real-time computer controller regulated air pressure in the artificial plantar flexor muscles proportional to the processed soleus electromyographic signals (EMG) via a pressure regulator. EMG signal from soleus was high-pass filtered with a second-order Butterworth filter (20-Hz cutoff frequency) to remove movement artifact, full wave rectified, and low-pass

filtered with a second-order Butterworth filter (10-Hz cutoff frequency) to smooth the signal.

Subjects completed two identical testing sessions approximately 72 hrs apart. During each session, subjects walked with the exoskeleton first without power for 10 min (baseline), with power for 30 min (powered), and without power again for 15 min (post-adaptation) (Gordon and Ferris 2007).

Data acquisition and analysis

We collected lower body kinematics, artificial muscle force, electromyography (EMG) and three-dimensional ground reaction forces (1200Hz) while subjects walked on a force-measuring split-belt treadmill (Collins et al. 2009) at 1.25 m/s. The three-dimensional kinematic data were collected by using an 8-camera video system (120 Hz, Motion Analysis Corporation, Santa Rosa, CA). Artificial muscle force data were collected with force transducers (1200 Hz, Omega Engineering) mounted on the bracket of exoskeleton. We estimated the amount of mechanical torque, power and work done by the exoskeleton using the measurement of artificial muscle moment arm and ankle kinematic data. We placed bipolar surface electrodes on the left lower limb to record EMG (1200 Hz, Konigsberg Instruments Inc.) from tibialis anterior (TA), soleus (SOL), medial gastrocnemius (MG), lateral gastrocnemius (LG). We used commercial software (Visual3D, C-Motion Inc., Germantown, MD) to calculate joint angles as well as joint kinetics by inverse dynamics analysis. Lower limb inertial properties were estimated based on anthropometric measurements of subjects (Zatsiorsky 2002) and the exoskeleton mass.

Ten seconds of data recorded each minute reflected the average of about seven strides of data. All data were time normalized to 100% of stride cycle (i.e., from left heel strike to left heel strike). To quantify changes in muscle activation, we calculated root-mean square (RMS) amplitude of the high-pass filtered (20-Hz cutoff frequency) and rectified EMG for the soleus over the stance phase. We normalized data to the last minute of baseline on a given testing session.

To examine changes in kinematics and kinetics across time for ankle, knee and hip joints, we linearly correlated the average joint angle and torque profiles during the powered condition at each minute to the average angle and torque profiles at the last minute of baseline on a given testing session using Pearson product moment correlation. The common variance (r^2) of the linear correlation was used as a quantitative measure of similarity in joint kinematics and torques between every minute's data and the data at the last minute of baseline (Derrick et al. 1994). To quantify variability of gait patterns in unpowered and powered walking, we calculated the coefficients of variation (CV) for joint angle and moment profiles (Winter 1991) during stance phase.

To compare the adaptation rate during powered walking to the single-muscle study (Gordon and Ferris 2007), we used the same method of quantifying motor adaptation (Noble and Prentice 2006) as the single-muscle study. An envelope of steady-state behavior during the powered walking was defined based on the mean±2SD of the final 15 minutes of day two if linear regression of the data in this period revealed slopes that were not statistically different from zero (t-test, $p > 0.05$). Statistically significant slopes of linear regression indicate

subjects did not reach steady state within the two training sessions. We calculated time to steady state for soleus stance RMS EMG, ankle joint correlation, and exoskeleton positive and negative mechanical work.

Statistics

We used repeated measure ANOVAs to test for differences in normalized EMG RMS (primary outcome variable was soleus stance RMS EMG), joint angle and torque correlation common variances (primary outcome variables were for the ankle joint), and positive and negative exoskeleton work between days and conditions (baseline, powered walking 1, 15, and 30) (2 days x 4 conditions). We analyzed other parameters as secondary outcome variables to provide insight into the overall adaptation. We set the significance level at $p<0.05$ and used Tukey Honestly Significant Difference (THSD) post hoc tests for pair-wise comparisons if a main effect was detected. We used paired t-test with Bonferroni correction to test for difference in the coefficients of variation (CV) of joint angle and moment profiles for hip, knee and ankle joints between baseline and minute 30 of day 2 (i.e. 6 comparisons).

Results

Joint Kinematics

Although subjects showed some adaptation over the two 30-minute sessions, there were still large differences in ankle joint kinematics at the end of the second session compared to baseline (Fig 2). When first walking with the exoskeleton assistance, subjects stayed at plantar flexed posture for almost the

whole gait cycle (Fig 2). Correspondingly, the ankle angle correlation common variance (r^2) at the first minute was the lowest during all testing (day 1, minute 1: 0.39±0.28, mean±SD) (Fig 4a). After 30 minutes of practice, subjects had similar ankle kinematics during mid-stance and swing but still had greater plantar flexion during mid-to-late stance compared to the baseline condition. The ankle angle correlation common variance (r^2) at minute 30 was significantly higher compared to the first minute (day 1, minute 30: 0.69±0.19, THSD, p<0.05). On the second day, ankle angle correlation common variance (r^2) at the minute 1 was significantly greater than the value during initial powered walking on day 1 (day2, minute 1: 0.63±0.19, THSD, p<0.05) and increased further with practice. However, the values of ankle angle correlation common variance were still significantly different from baseline by the end of day 2 (day 2, min 30: 0.79± 0.12, THSD, p<0.05).

There were no large differences in knee or hip joint kinematics during powered walking. Throughout the active trials, knee and hip angle correlation common variances were always greater than 0.96 and 0.97, respectively. On the second day, there were no significant differences between minute 30 and baseline (THSD, p>0.05) in joint angle correlation common variances for knee (day 2, min 30: 0.98± 0.01) or hip (0.99± 0.01) after 30 minutes of training.

Joint kinetics

Hip, knee and ankle joint moment profiles at the end of each session were only slightly different compared to the baseline while these small changes resulted in a larger difference in the overall support moment (Fig 3). The values

of ankle (Fig 4b), knee and hip moment correlation common variance (r^2) were the lowest at minute 1 (ankle: 0.85±0.13; knee: 0.77±0.23, hip: 0.96±0.03). With practice, the correlation common variances (r^2) of joint moment profiles increased during the second session. By the end of day 2, subjects walked with similar total joint moment profiles during the powered condition as during the baseline condition (Fig 3). Joint moment correlation common variances (r^2) for hip (0.98±0.01), knee (0.90±0.16), or ankle (0.98±0.02) at minute 30 of day 2 were not significantly different from the baseline (THSD, p>0.05).

Subjects walked with similar knee and hip joint power profiles but very different ankle joint power profiles (Fig 6) and ankle work during the powered condition. After 30 minutes of training, subjects had greater power generation and less power absorption at the ankle joint on both days. Compared to the baseline, the peak ankle positive power in the powered condition was significantly greater at the end of day 2 (baseline: 152.93± 29.38 W; day 2, minute 30: 203.04±64.90 W, p=0.015). In addition, the total ankle positive work was significantly greater than the ankle positive work at the baseline by ~66% (baseline: 13.07±2.94 J; day 2, minute 30: 21.74±6.83 J, THSD, p<0.05); and the total ankle negative work was ~51% less than the ankle negative work at the baseline (baseline: -15.68±4.27 J; day 2, minute 30: -7.66±4.01 J, THSD, p<0.05).

Electromyography (EMG)

Subjects had substantially smaller soleus EMG activation during powered walking (Fig 5). By the end of day 2, soleus stance RMS EMG amplitude (0.64±

0.14) was significantly lower than the baseline by ~36% (THSD, $p<0.05$) (Fig 5b). For other lower limb muscles, the muscle activation patterns were similar to the baseline by the end of training.

Exoskeleton mechanics

The powered exoskeleton with double muscles provided substantial assistance (Fig 3 and 6). The peak plantar flexor torque provided by the exoskeleton (50.09±12.05 Nm) was ~43% of peak ankle plantar flexor moment at the baseline (116.48±26.10 Nm), and ~47% of peak ankle plantar flexor moment at minute 30 (107.14±23.56 Nm) on day 2 (Fig 3). The peak mechanical power generated by the exoskeleton was 117 W, about 80% of peak positive ankle joint power at the baseline (147.2±32.97 W), and ~61% of peak ankle joint power at minute 30 (191.59±64.57 W) (Fig 6).

Coefficient of variation (CV)

Subjects had significantly greater variability in ankle joint angle profile during powered than during unpowered walking. Compared to the baseline, subjects had larger coefficients of variation both in joint angle and moment profiles during powered walking. There were significant differences in the coefficients of variation for ankle angle profiles between baseline and minute 30 of the powered condition (baseline: 0.14±0.04; minute 30: 0.30±0.12, $p=0.0008<0.0083$) but not for ankle moment profiles (baseline: 0.13±0.02; minute 30: 0.17±0.05, $p=0.07>0.0083$) after two sessions of training.

Adaptation period

Not all of the subjects reached steady state dynamics within two training sessions compared to the 100% success rate in the study of single muscle design (Gordon and Ferris 2007). The significant slope of linear regression on the data of last 15 minutes of day 2 indicated that five out of eleven subjects did not reach steady state dynamics in soleus RMS EMG.

Discussion

The findings of this study support our hypothesis that subjects would walk with similar joint moment patterns during powered versus unpowered walking. When the robotic assistance was provided, subjects reduced soleus EMG activation by about 36% to walk with a similar total ankle moment pattern (biological plus exoskeleton moment). However, they walked with a substantially different ankle kinematic pattern compared to the unpowered condition. In addition, the variability of ankle moment profile was similar during powered versus unpowered walking while the variability of ankle angle profile was significantly greater in the powered condition. The results indicate that humans seem to adopt invariant ankle moment patterns with and without robotic lower limb assistance.

Another finding of this study is that subjects had significantly different overall support moment at late stance during powered versus unpowered walking. The reduction in the second peak of overall support moment resulted from a small decrease in plantar flexor moment and an increase in knee flexor moment. We found that subjects had slightly greater horizontal ground reaction

forces and similar vertical ground reaction forces at late stance in the powered condition. During powered walking, the slight reduction in ankle plantar flexor moment might result from more plantar flexed ankle position at late stance while an increase in knee flexor moment might be caused by the greater horizontal ground reaction forces. This finding suggests that overall support moment pattern is not as consistent with robotic lower limb assistance as has been found without lower limb assistance (Winter 1980; Winter 1989).

The powered ankle exoskeleton replaced some of the ankle plantar flexor torque and did not substantially alter the dynamics of the other joints. One of the primary goals for robotic lower limb exoskeletons is to replace some of the mechanical work required for walking in order to reduce metabolic expenditure. The results showed that joint moment profiles of ankle, knee and hip were similar during powered versus unpowered walking. This is particularly notable given that the ankle exoskeleton was providing ~47% of the total ankle joint moment at push-off during the powered condition. This finding supports the concept that a joint kinetic rule of inter-limb coordination may be used in the neural control of human gait (Shemmell et al. 2007).

Our results also have important implications for training people to use robotic lower limb assistance during locomotion. Only about half of our subjects reached steady state muscle activation patterns after two 30-minute training sessions. This is in contrast to what was found on a robotic ankle exoskeleton with less mechanical capability (Gordon and Ferris 2007). Gordon and Ferris (2007) found that their subjects had reached steady state at about 15 minutes of

training on the second day. This difference between studies supports the hypothesis that subjects take longer time to reach steady state dynamics when walking with robotic exoskeleton of greater mechanical capability. Subjects likely increased their co-activation and joint impedance when initially dealing with robotic assistance that greatly perturbed the movement dynamics (e.g., greater muscle activation was shown for other leg muscles such as TA, VM, VL, RF and MH during powered walking). Although EMG activation of other leg muscles became similar to the baseline by the end of training, the increased joint impedance during initial powered walking might slow down the adaptation process.

Acknowledgments

The authors thank Kristin Carroll, Danielle Sandella, Evelyn Anaka, and members of the Human Neuromechanics Laboratory for assistance in collecting data. We also thank Anne Manier for help with fabricating the exoskeleton. Supported by NIH R21 NS062119 (DPF) and F32 HD055010 (CLL).

Figures

Figure 3.1 Powered ankle exoskeleton.
Subjects wore a custom made exoskeleton on their left lower limb. The exoskeleton consisted of a carbon fiber shank section and a polypropylene foot section. The exoskeleton was hinged at the ankle to allow free sagittal plane rotation. The exoskeleton had an average weight of 1.08±0.09 kg (mean±SD) and moment arm length of 11.0±1.2 cm that varied and depended on the size of the subject. Electrical signals (EMG) of soleus were recorded and processed to be used to control air pressure in the artificial pneumatic muscles proportionally. As air pressure increased, the artificial muscles started to develop tension and become shortened, allowing the powered exoskeleton to provide plantar flexor torque controlled by soleus muscle activation.

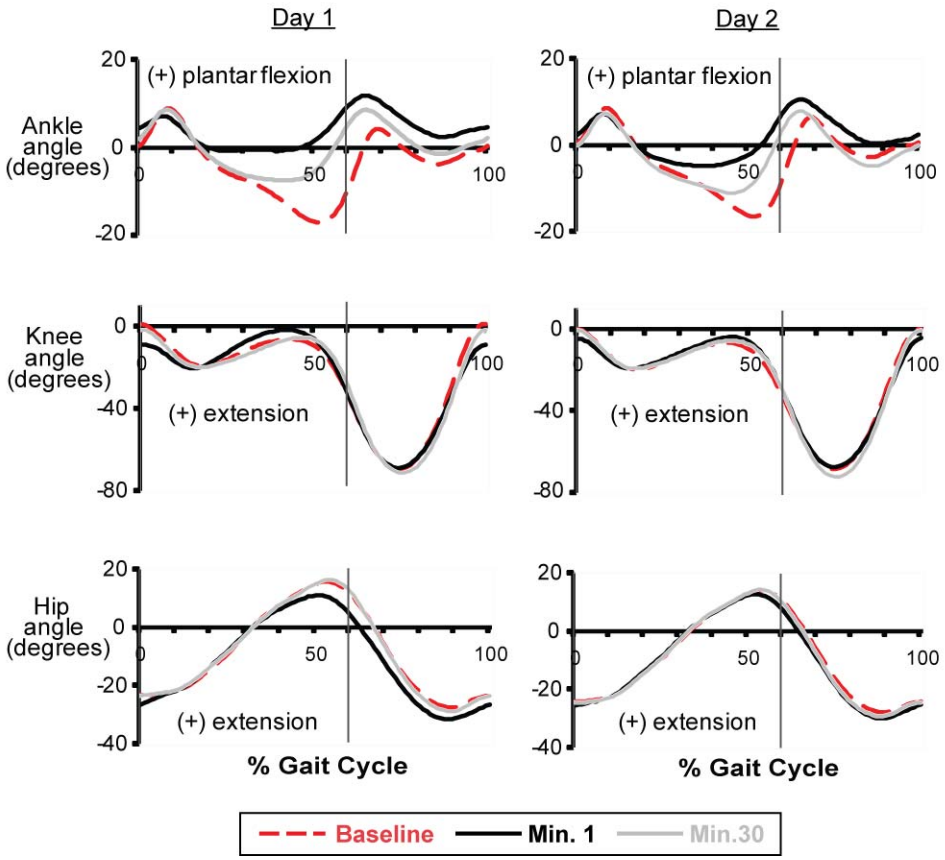

Figure 3.2 Joint kinematics.
Ankle, knee and hip joint angle profiles are shown for the last minute of baseline condition (baseline, red dashed line), the first minute of active condition (minute 1, black line), and the last minute of active condition (minute 30, grey line) on the two training sessions. Data are the average of all subjects. The vertical lines represent the toe-off. Positive values indicate ankle plantar flexion, knee extension and hip extension. Compared to the baseline, the ankle joint angle profiles showed greater plantar flexion during mid-to-late stance during powered walking. The hip and knee joint angle profiles were similar to the baseline by the end of training of each day.

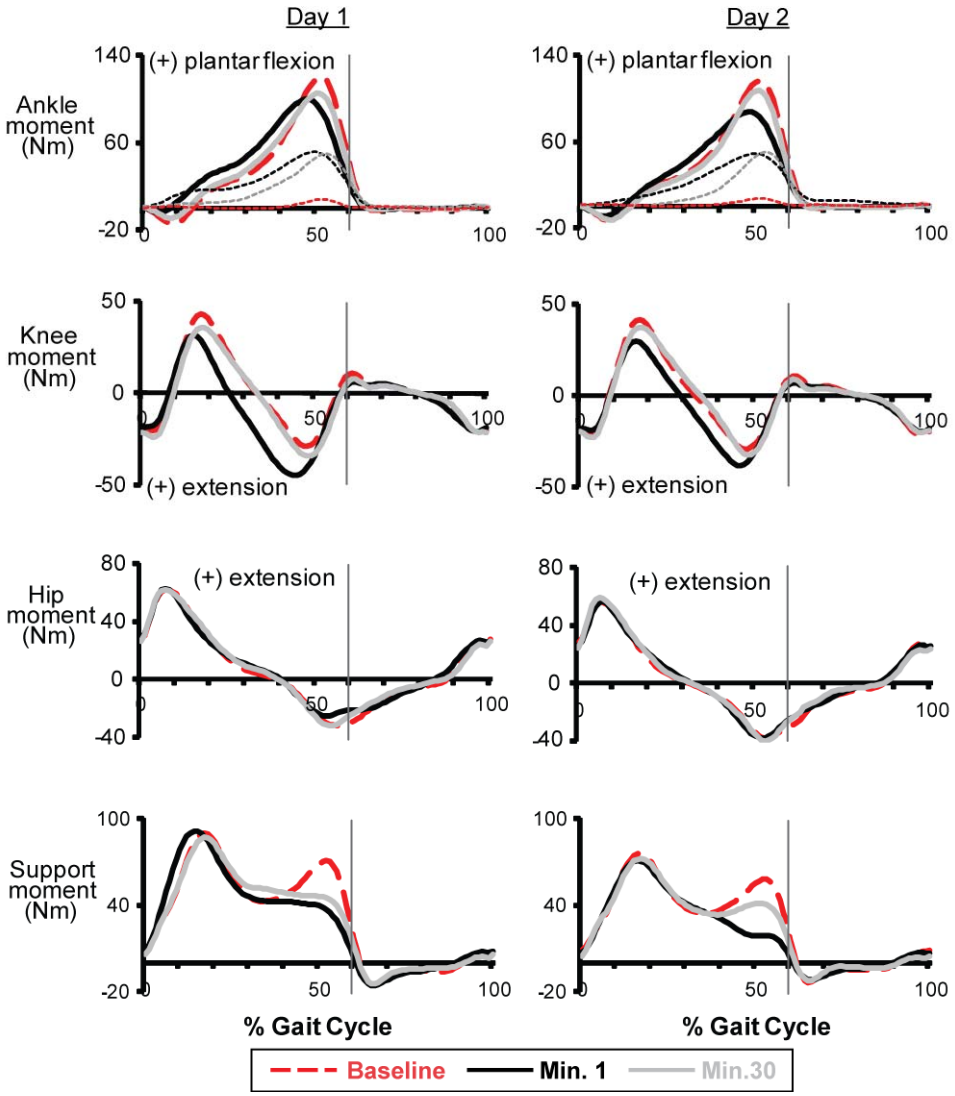

Figure 3.3 Joint moments, overall support moment, and exoskeleton mechanical torque.
The thicker lines represent the ankle, knee, hip and overall support moment (i.e., sum of the extensor moments across the hip, knee and ankle joints) profiles on the two training sessions. The thinner dashed lines with the ankle joint moment data represent the plantar flexor torque provided by the exoskeleton (calculated from artificial muscle force and muscle moment arm) at the baseline (red), active minute 1 (black) and active minute 30 (grey). Data are the average of all subjects. At the end of day 2, the peak torque provided by the exoskeleton (50.09±12.05 Nm) was ~43% of peak ankle joint moment at the baseline (116.48±26.10 Nm) or ~47% of peak ankle joint moment at the minute 30 (107.14±23.56 Nm). After two sessions of training, the individual joint moment profiles were similar to the baseline. However, the second peak of overall support moment was smaller than the baseline on day two (baseline: 58.86±12.90 Nm, minute 30: 46.44±17.09 Nm).

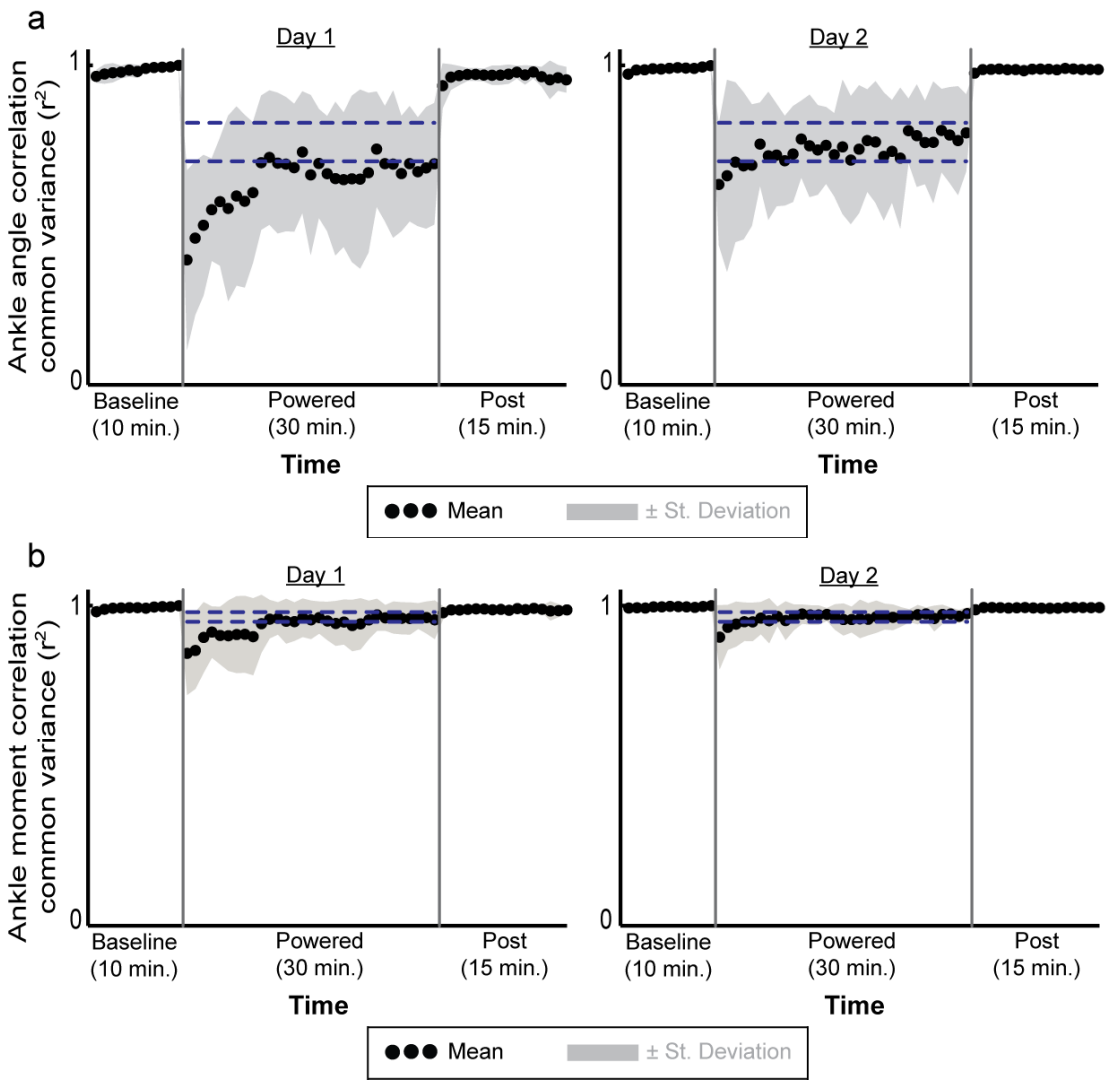

Figure 3.4 Ankle joint angle (a) and moment (b) correlation common variance (r^2).
Mean data (black dots) ± 1 standard deviation (grey area) are shown for each minute. The two horizontal blue lines are the mean±2 standard deviations from the last 15 minutes of active condition on day2, representing steady state dynamics. The steady state envelopes shown above from the average group data are for display purposes. Steady state dynamics were determined for each subject, individually. The values of correlation common variance (r^2) increased with practice in the active condition both for joint angle and moment. By the end of active condition on day 2 (day 2, minute), the values of correlation common variance were similar to the baseline for ankle moment profile (0.98±0.02, THSD, p>0.05) but not for ankle angle profile (0.79±0.12, THSD, p<0.05).

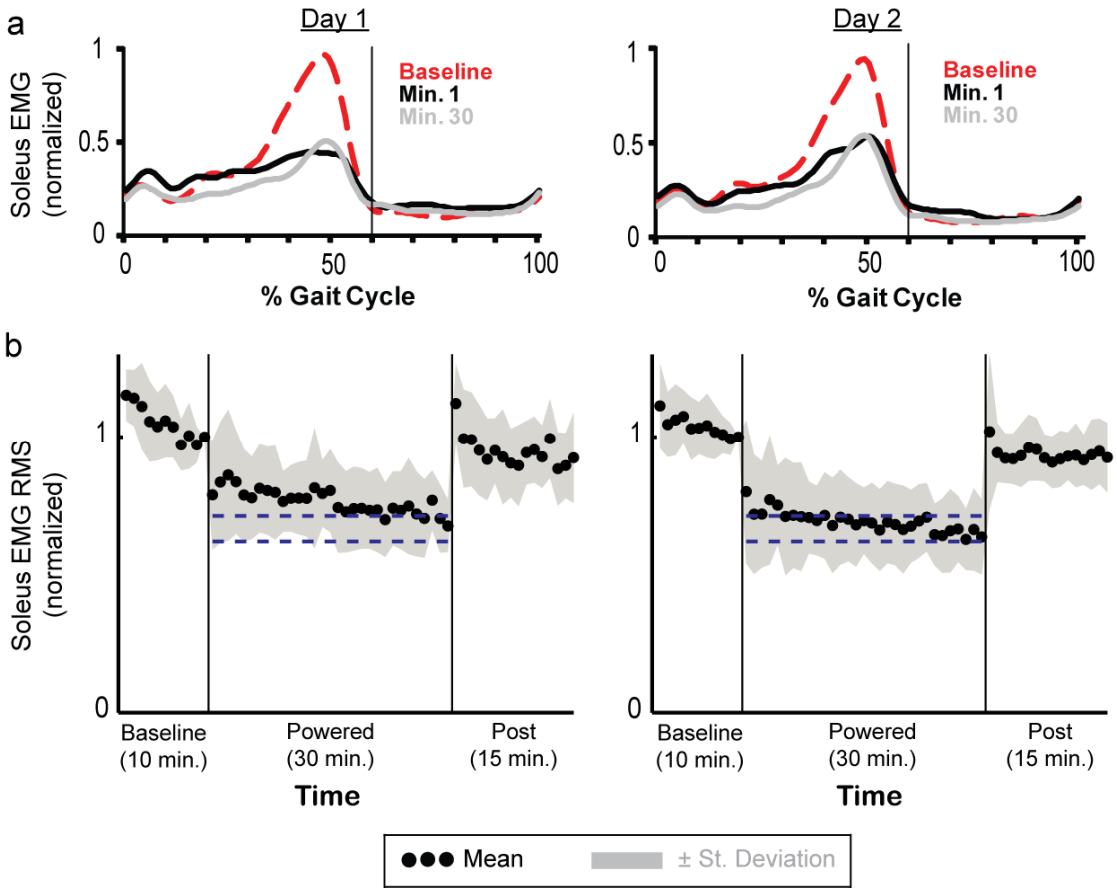

Figure 3.5 Soleus activation patterns (a) and soleus stance EMG RMS amplitudes (b).
(a) Soleus EMG linear envelopes (rectified and low-pass filtered EMG with 6-Hz cutoff frequency) were averaged from all subjects. During initial walking with the powered exoskeleton (day 1, minute 1), subjects had lower soleus activation right away. After 30 minutes of practice, soleus activation pattern showed a clear bursting shape similar to the baseline. (b) Soleus EMG RMS amplitudes during stance. Mean data (black dots)±1 standard deviation (grey area) are shown for each minute. The two horizontal blue lines are the mean±2 standard deviation from the last 15 minutes of active condition on day 2, representing steady state dynamics. The steady state envelopes shown above from the averaged group data are for display purposes. Steady state dynamics were determined by each subject, individually. By the end of day 2 (day 2, minute 30), the soleus stance EMG RMS amplitude was reduced by ~36% (0.64±0.14) compared to the baseline.

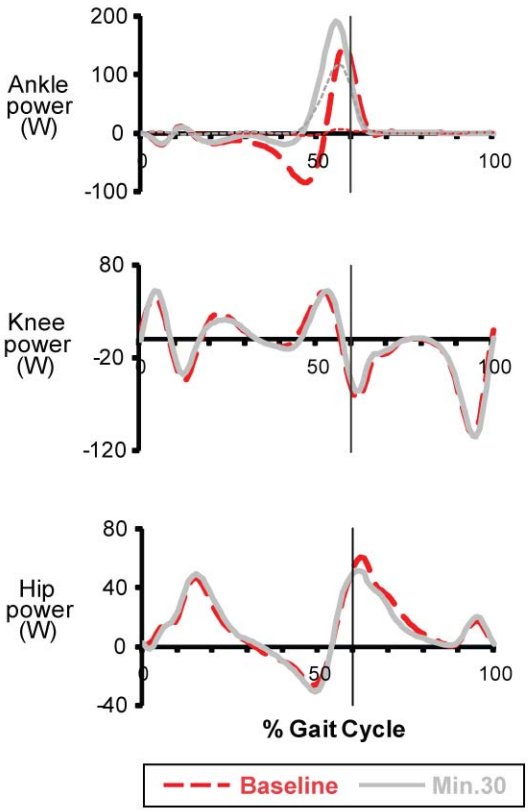

Figure 3.6 Joint powers and the mechanical power provided by the exoskeleton on day 2.
The thicker lines represent the ankle, knee and hip joint power profiles. The thinner dashed line with the ankle joint power data represent the mechanical power provided by the exoskeleton (calculated from artificial muscle force, muscle moment arm and ankle joint velocity) at the baseline (red) and powered minute 30 (grey). Data are the average of all subjects. After two sessions of training, joint power profiles were similar to the baseline except the ankle joint power profile. Throughout the powered condition, subjects had greater power generation and less power absorption at the ankle joint. The exoskeleton produced a peak positive mechanical power of 117 W, about 80% of peak positive ankle joint power at the baseline (147.2±32.97 W) or ~61% of peak ankle joint power at the minute 30 (191.59±64.57 W).

References

Cain SM, Gordon KE, Ferris DP (2007) Locomotor adaptation to a powered ankle-foot orthosis depends on control method. Journal of Neuroengineering and Rehabilitation 4

Collins SH, Adamczyk PG, Ferris DP, Kuo AD (2009) A simple method for calibrating force plates and force treadmills using an instrumented pole. Gait & Posture 29: 59-64

Derrick TR, Bates BT, Dufek JS (1994) Evaluation of Time-Series Data Sets Using the Pearson Product-Moment Correlation-Coefficient. Medicine and Science in Sports and Exercise 26: 919-928

Dollar AM, Herr H (2008) Lower extremity exoskeletons and active orthoses: Challenges and state-of-the-art. Ieee Transactions on Robotics 24: 144-158

Ferris DP, Czerniecki JM, Hannaford B (2005a) An ankle-foot orthosis powered by artificial pneumatic muscles. Journal of Applied Biomechanics 21: 189-197

Ferris DP, Gordon KE, Sawicki GS, Peethambaran A (2006) An improved powered ankle-foot orthosis using proportional myoelectric control. Gait and Posture 23: 425-428

Ferris DP, Sawicki GS, Daley MA (2007) A physiologist's perspective on robotic exoskeletons for human locomotion. International Journal of Humanoid Robotics 4: 507-528

Ferris DP, Sawicki GS, Domingo A (2005b) Powered lower limb orthoses for gait rehabilitation. Topics in Spinal Cord Injury Rehabilitation 11: 34-49

Gordon KE, Ferris DP (2007) Learning to walk with a robotic ankle exoskeleton. Journal of Biomechanics 40: 2636-2644

Gordon KE, Sawicki GS, Ferris DP (2006) Mechanical performance of artificial pneumatic muscles to power an ankle-foot orthosis. Journal of Biomechanics 39: 1832-1841

Kinnaird CR, Ferris DP (2009) Medial gastrocnemius myoelectric control of a robotic ankle exoskeleton for human walking. IEEE Transactions on Neural Systems and Rehabilitation Engineering 17: 31-37

Lelas JL, Merriman GJ, Riley PO, Kerrigan DC (2003) Predicting peak kinematic and kinetic parameters from gait speed. Gait & Posture 17: 106-112

Noble JW, Prentice SD (2006) Adaptation to unilateral change in lower limb mechanical properties during human walking. Experimental Brain Research 169: 482-495

Prilutsky BI, Sirota MG, Gregor RJ, Beloozerova IN (2005) Quantification of motor cortex activity and full-body biomechanics during unconstrained locomotion. Journal of Neurophysiology 94: 2959-2969

Sawicki GS, Ferris DP (2008) Mechanics and energetics of level walking with powered ankle exoskeletons. Journal of Experimental Biology 211: 1402-1413

Sawicki GS, Ferris DP (2009a) Mechanics and energetics of incline walking with robotic ankle exoskeletons. Journal of Experimental Biology 212: 32-41

Sawicki GS, Ferris DP (2009b) Powered ankle exoskeletons reveal the metabolic cost of plantar flexor mechanical work during walking with longer steps at constant step frequency. Journal of Experimental Biology 212: 21-31
Shemmell J, Johansson J, Portra V, Gottlieb GL, Thomas JS, Corcos DM (2007) Control of interjoint coordination during the swing phase of normal gait at different speeds. Journal of Neuroengineering and Rehabilitation 4
Winter DA (1980) Overall principle of lower limb support during stance phase of gait. Journal of Biomechanics 13: 923-927
Winter DA (1989) Biomechanics of Normal and Pathological Gait - Implications for Understanding Human Locomotor Control. Journal of Motor Behavior 21: 337-355
Winter DA (1991) The biomechanics and motor control of human gait: normal, elderly and pathological. Waterloo Biomechanics, Waterloo, Ontario
Winter DA, Eng P (1995) Kinetics: our window into the goals and strategies of the central nervous system. Behavioural Brain Research 67: 111-120
Zatsiorsky VM (2002) Kinetics of Human Motion. Human Kinetics, Champaign, IL

Chapter IV

Short-term locomotor adaptation to a robotic ankle exoskeleton does not alter soleus Hoffmann reflex amplitude

Abstract

To design better robotic lower limb exoskeletons for gait rehabilitation, it is critical to identify neural mechanisms that govern locomotor adaptation to robotic assistance. Previously, we demonstrated soleus muscle recruitment decreased by ~35% when walking with a pneumatically-powered ankle exoskeleton providing plantar flexor torque under soleus proportional myoelectric control. Since a substantial portion of soleus activation during walking results from the stretch reflex, increased reflex inhibition is one potential mechanism for reducing soleus recruitment when walking with exoskeleton assistance. This is clinically relevant because many neurologically impaired populations have hyperactive stretch reflexes and training to reduce the reflexes could lead to substantial improvements in their motor ability. The purpose of this study was to quantify soleus reflex responses during powered versus unpowered walking. We tested soleus Hoffmann (H-) reflex responses in neurologically intact subjects (n=8) that had trained walking with the robotic ankle exoskeleton. We found that subjects had similar H-reflex amplitude in proportion to the background soleus EMG

during powered walking versus unpowered walking (p>0.05). These findings suggest that the nervous system does not change the gain of the soleus stretch reflex in response to short-term adaption to exoskeleton assistance. Future studies should determine if the findings also apply to long-term adaption to the exoskeleton.

Key words: H-reflex, motor adaptation, powered orthosis, human walking

Introduction

Many research groups are developing robotic lower limb exoskeletons to assist in locomotion training after neurological injury (Colombo et al. 2001; Wirz et al. 2001; Werner et al. 2002; Sawicki et al. 2006; Banala et al. 2007; Emken et al. 2008). The exoskeletons are intended to reduce manual effort from therapists and improve rehabilitation outcomes. Though reducing manual effort from therapists is clearly being achieved by current devices, results for achieving better rehabilitation outcomes are still equivocal. Studies have demonstrated that the choice of computer control algorithms for robotic gait devices can affect the process of motor learning to robotic assistance (Sawicki et al. 2006; Aoyagi et al. 2007; Cain et al. 2007; Emken et al. 2007; Edgerton and Roy 2009; Reinkensmeyer and Patton 2009). However, there is no clear theory on how different control algorithms specifically alter mechanisms or aspects of neural control (Huang and Krakauer 2009; Crespo and Reinkensmeyer In press). To

design better robotic gait devices that can enhance therapy, it is critical to identify neural mechanisms that govern locomotor adaptation to robotic assistance.

In a recent study from our laboratory, Gordon and Ferris examined how healthy young subjects adapted to a robotic ankle exoskeleton during walking (Gordon and Ferris 2007). The exoskeleton provided plantar flexor torque under proportional myoelectric control of soleus electromyographic (EMG) activation. When the robotic assistance was first introduced, subjects walked with extreme plantar flexion during stance. After two thirty-minute training sessions three days apart, subjects had reduced soleus muscle activation by ~35% and walked smoothly with the exoskeleton mechanical assistance. A large portion of soleus muscle activation is a direct result of proprioceptive feedback, including the stretch reflex response (Yang et al. 1991b; Sinkjaer et al. 1996; Nielsen and Sinkjaer 2002; Mazzaro et al. 2005a; Mazzaro et al. 2005b; Rossignol et al. 2006; af Klint et al. 2008; af Klint et al. 2009). Thus, the nervous system could inhibit this feedback reflex activation during walking with the exoskeleton as a mechanism for reducing soleus recruitment.

Increased stretch reflex inhibition with robotic exoskeleton training would be particularly relevant to gait rehabilitation for individuals after neurological injuries. Individuals who had stroke, spinal cord injury, cerebral palsy, and traumatic brain injury often demonstrate abnormally high stretch reflexes that substantially affect their movement capabilities (Yang et al. 1991a; Dietz 2001; Dietz 2002; Phadke et al. 2007). A number of research groups have been investigating training methods to inhibit reflexes and their results demonstrated

that reflex responses can be manipulated both in patient populations (Trimble et al. 1998; Trimble et al. 2001; Chen et al. 2006; Phadke et al. 2007) and neurologically intact subjects (Trimble and Koceja 1994; Mynark and Koceja 2002; Schneider and Capaday 2003; Mazzocchio et al. 2006). Chen et al (2006) concluded that conditioning of reflex responses in a rat model can improve functional locomotion after spinal cord injury (Chen et al. 2006). If a robotic exoskeleton could be used to induce an alteration of reflex responses during human walking, it would have considerable potential as an aid for gait rehabilitation.

The purpose of this study was to quantify soleus reflex responses in neurologically intact subjects trained to walk with the robotic ankle exoskeleton. We used the Hoffmann (H-) reflex, an electrical analog of the stretch reflex, to examine soleus reflex responses during walking both with the exoskeleton powered and with the exoskeleton unpowered. The H-reflex is elicited by stimulating the afferent nerve (Ia sensory) directly and bypassing the muscle spindle. H-reflex measurements have been extensively used to study how the stretch reflex is modulated centrally (Romano and Schieppati 1987; Sinkjaer 1997; Schneider et al. 2000; Ferris et al. 2001; Knikou 2008). The H-reflex is highly task-dependent and is modulated frequently during motor behaviors (Capaday and Stein 1986; Stein and Capaday 1988; Dyhre-Poulsen et al. 1991; Simonsen and Dyhre-Poulsen 1999; Dyhre-Poulsen and Simonsen 2001; Ferris et al. 2001). A reduction in H-reflex amplitude has been associated with mastering new motor tasks such as balancing during standing (Trimble and

Koceja 1994; Mynark and Koceja 2002), perturbed cycling (Mazzocchio et al. 2006), and backward walking tasks (Schneider and Capaday 2003; Ung et al. 2005). In a pilot study, a single subject that had trained with the ankle exoskeleton for several years demonstrated a much lower H-reflex amplitude in proportion to the background EMG during powered walking compared to during unpowered walking (Ferris and Kinnaird 2008). Based on that finding, we hypothesized that subjects would have lower H-reflex magnitudes when normalized to background soleus activity during adapted powered walking than during unpowered walking. In this study, we tested eight subjects who had trained to walk with the robotic ankle exoskeleton for two training sessions.

Methods

Subjects

Eight healthy, neurologically intact subjects (4 male, 4 female) gave written informed consent and participated in the study. The University of Michigan Medical School Institutional Review Board approved the protocol, and the study conformed to the standards set by the Declaration of Helsinki.

Experimental design and protocol

We constructed a custom-made orthosis (Fig. 1) for the left lower limb of each subject. The exoskeleton consisted of a carbon fiber shank section and a polypropylene foot section. A metal hinge between the sections allowed free sagittal plane rotation of the ankle joint. Two artificial pneumatic muscles attached to the brackets mounted on the exoskeleton provided substantial

plantar flexor torque. Details of the design and performance of the exoskeleton are documented elsewhere (Ferris et al. 2005; Ferris et al. 2006; Gordon et al. 2006). We implemented proportional myoelectric control (i.e., amplitude and timing) of the artificial muscles through desktop computer and real-time control board (dSPACE Inc.). A custom real-time computer controller regulated air pressure in the artificial plantar flexor muscles proportional to the processed soleus electromyographic signals (EMG) via a pressure regulator. EMG signal from the soleus muscle was high-pass filtered with a second-order Butterworth filter (20-Hz cutoff frequency) to remove movement artifact, full wave rectified, and low-pass filtered with a second-order Butterworth filter (10-Hz cutoff frequency) to smooth the signal. Adjustable gains scaled the control signals and a threshold cutoff eliminated background noise.

Before the testing of soleus H-reflex, subjects had completed two 30-minute treadmill training sessions for walking with the powered ankle exoskeleton controlled by soleus EMG (Gordon and Ferris 2007). Soleus H-reflex was tested while subjects walked with the exoskeleton first without power (first unpowered), then with power (powered), and finally without power again (second unpowered) on the treadmill at 1.25 m/s. The second unpowered condition was for monitoring the influence of multiple stimulations on the H-reflex amplitudes (e.g., homosynaptic or post-activation depression).

Data acquisition and analysis

We collected lower body kinematics, artificial muscle force, electromyography (EMG) and ground reaction forces while subjects walked on a

custom-constructed force-measuring split-belt treadmill at 1.25 m/s. The three-dimensional kinematic data were collected by using 8-camera video system (120 Hz, Motion Analysis Corporation, Santa Rosa, CA) with reflective markers. Artificial muscle force data were collected with force transducers (1200 Hz, Omega Engineering) mounted on the bracket of orthosis. We placed bipolar surface electrodes on the left shank to record EMGs (1200 Hz, Konigsberg Instruments Inc.) from tibialis anterior (TA), soleus (SOL), medial gastrocnemius (MG), lateral gastrocnemius (LG).

Soleus H-reflex measurements

We elicited the soleus H-reflex by stimulating (DS7AH constant current stimulator, Digitimer Ltd.) the tibial nerve with a cathode placed in the popliteal fossa and an anode (7-cm diameter) on the patella. The electrical stimulus was 1-millisecond monophasic square pulse. To locate the optimal nerve stimulation site, we delivered a couple of stimuli on different spots in the popliteal fossa. The criterion for choosing the site of cathode placement was the largest M-wave amplitude at a constant intensity of stimulation. Before the walking trials, we measured the peak-to-peak amplitudes of M and H waves from surface electrodes (2000 Hz) across different stimulation intensities to gather a standing H-reflex and M-wave recruitment curve while subjects were standing motionless with the ankle exoskeleton unpowered.

For the walking trials, we tested the soleus H-reflex in the 3 conditions (first unpowered, powered and second unpowered). We divided the gait cycle into 16 equal epochs (10 epochs in the stance). To reduce the effects of a large

number of stimuli on the reflex response, we evoked soleus H-reflexes for only three epochs: two during mid-stance (epoch 5 and 6) and one during late stance (epoch 8). We used a custom-written program and a real-time control board (dSPACE Inc.) to control the timing of electrical stimuli and to measure the resulting M-wave and H-wave peak-to-peak amplitudes (2000 Hz). We randomly dispersed the stimuli to each of the 3 epochs. The program sent a stimulus at least every 4 seconds.

The size of the M-wave as a percentage of the maximal M-wave (i.e., M_{max}, maximal evoked muscle response) has been used regularly to control constant effective stimulus intensity to the afferent nerve (Capaday 1997; Simonsen and Dyhre-Poulsen 1999; Ferris et al. 2001). Stimulating to produce an M-wave that is a constant percentage of M_{max} results in the recruitment of approximately the same number of motor axons, indicating that stimulus intensity to the afferent nerve is also constant (Capaday and Stein 1986). While walking, the relative movement between stimulating electrode and the nerve may change M_{max} over a stride (Simonsen and Dyhre-Poulsen 1999). To account for changes in M_{max}, we first collected M_{max} data (~3 M_{max} measurements) of each epoch by delivering a larger stimulus than the one evoked M_{max} during quiet standing (at least 1.2 times of stimulation intensity for evoking M_{max} during quiet standing). This provided us a measure of M_{max} at the 3 time points of gait cycle.

The effective stimulus intensity used for the H-reflex measurements was the intensity to evoke a corresponding M-wave that is 25% of M_{max} for that epoch. The program monitored the peak-to-peak amplitude of the M-wave

produced by the stimulus, and calculated the ratio of the M-wave amplitude to the M_{max} of that epoch. We only accepted H-reflex measurements where the M-wave was 25 ± 10% of the corresponding M_{max}. To ensure constant stimulus intensity over the gait cycle, we manually adjusted the intensity of subsequent stimuli if the ratio was not within the range of 25 ± 10%. We collected 10 measurements of H-reflex where the corresponding M-wave was 25 ± 10% of M_{max} in each epoch.

For background soleus EMG amplitudes, we calculated the mean of rectified averaged soleus EMG of each time epoch. We normalized the H-reflex amplitudes and mean EMG measurements to the M_{max} for that time epoch. This procedure corrected for changes in H-reflex and background EMG values due to movement for the muscle fibers relative to the recording electrodes (Simonsen and Dyhre-Poulsen 1999). Since the H-reflex amplitude depends on the background level of motor activity (Capaday and Stein 1987; Capaday 1997), we calculated the ratio of H-reflex amplitude to its corresponding background EMG amplitude. To reduce the inter-subject variability, we then normalized the H-reflex, mean EMG amplitudes and the ratio between H-reflex and background EMG in each condition to the values of the first unpowered condition.

Statistical analysis

We performed multiple one-way ANOVAs to test for differences in normalized H-reflex amplitudes, soleus EMG amplitudes and the ratio between H-reflex and background EMG at the three epochs between the three conditions (first unpowered, powered, and second unpowered). We set the significance level at $p<0.05$ and used Bonferroni correction. If a main effect was detected, we

used Tukey Honestly Significant Difference (THSD) post hoc tests for pair-wise comparisons. All statistical analyses were performed in JMP statistical software (SAS institute Inc., Cary, NC, USA).

Results

When the robotic plantar flexor torque was provided, subjects walked with decreased soleus EMG but different ankle joint kinematics at late stance (Fig. 2). Compared to the unpowered condition, subjects had similar ankle joint angle profiles during initial to middle stance but the ankle angle profiles deviated from the unpowered ankle angle profiles at epoch 7 (Fig. 2A). In addition, the soleus activation was significantly lower in the powered condition (epoch 5: 0.60±0.17, p=0.0002; epoch 6: 0.52±0.20, p=0.0002; epoch 8: 0.73±0.22, p=0.0316) than the two unpowered conditions (Fig. 2B, Fig. 3B). The soleus EMG amplitudes as well as H-wave amplitudes in the first unpowered condition were 1 (100%) for the three epochs because we normalized the data in each condition to the first unpowered condition.

The reduction in soleus EMG activation was much more than the reduction in H-wave amplitude during powered walking. Subjects had significantly lower H-wave amplitudes at epoch 5 (0.76±0.13, p=0.0035) and 6 (0.80±0.22, p=0.0059) but not at epoch 8 (0.88±0.46, p=0.51) during powered walking (Fig. 3A). Compared to 27-48% of decrease in soleus EMG activation, H-wave amplitudes were only lowered by 12-24% in the powered condition. Thus, the ratio of H-wave amplitude and background soleus EMG amplitude during

powered walking were not significantly (p>0.05) greater (epoch 5: 1.33±0.26, epoch 6: 1.62±0.60, epoch 8: 1.11±0.67) compared to the unpowered conditions (Fig. 3C).

Discussion

Our findings do not support the hypothesis that the normalized amplitude of soleus H-reflex is reduced when training with a robotic ankle exoskeleton under soleus proportional myoelectric control. With short term training, our subjects reduced soleus background EMG by ~35% and had concomitant reductions in H-reflex amplitude by ~20% during steady-state powered walking. As a result, subjects demonstrated slightly higher H-reflex amplitude relative to their background muscle activity compared to unpowered walking. The unaltered H-reflex modulation indicates that stretch reflex inhibition is not one of the mechanisms for reducing soleus EMG when adapting to robotic assistance with short term training. Instead, our results suggest that mechanisms for this short-term adaptation to the robotic assistance could be increased inhibition of the motor neuron or a reduction in supra-spinal drive (Wolpaw 1997).

Adaptation to the robotic exoskeleton assistance during walking may occur in two phases, a quick adaptation that occurs in the first few hours or days and a much longer adaptation that continues for weeks (Wolpaw and Okeefe 1984; Luft and Buitrago 2005; Bastian 2008). The two adaptation phases may have been reflected by the difference between our current study results on newly trained subjects and the pilot study on a long-term trained subject (Ferris and

Kinnaird 2008). When initially walking with the robotic ankle exoskeleton, subjects' gait patterns were greatly disturbed by the additional ankle mechanical torque provided (Gordon and Ferris 2007). Decreased motor output of soleus motor neurons due to increased post-synaptic inhibition or a reduction in supra-spinal excitation (Shefchyk and Jordan 1985) would be strategies to quickly reduce soleus EMG without altering the excitability of the reflex pathway. With longer term training, modulation of spinal reflex pathways by supra-spinal centers (i.e., increased pre-synaptic inhibition of Ia afferents) could contribute to soleus EMG reduction without need for constant supraspinal inhibition. The different sensorimotor calibration after long term training may result from repeated motor adaptation to the robotic assistance (Bastian 2008).

During the initial learning of a motor task, increased attention may also enhance the reflex responses. Previous studies have shown greater H-reflex responses during the initial training on a novel locomotion task such as obstacle avoidance during walking (Hess et al. 2003) and backward walking (Schneider and Capaday 2003). In our study, the subjects had trained with the robotic-assisted walking for two thirty-minute sessions and had at least 15-minute of warm-up in powered walking by the time of H-reflex testing. However, from subjects' reports and our observations, a certain amount of attention or concentration was still necessary to walk smoothly with the augmented mechanical plantar flexor torque provided by the exoskeleton at the third session. This may have contributed to the enhanced H-reflex amplitude relative to the background EMG in our study.

Conclusion

After short-term training in walking with the ankle exoskeleton, subjects had similar soleus Hoffmann-reflex amplitude in proportion to the background muscle activation during powered versus unpowered walking. These findings indicate that the nervous system did not alter reflex responses as the mechanism for reducing soleus recruitment during short term adaptation. Future studies should determine if the findings also apply to long-term adaption to the exoskeleton.

Acknowledgments

The authors thank Evelyn Anaka, Danielle Sandella, Catherine Kinnaird and members of the Human Neuromechanics Laboratory for assistance in collecting data. We also thank Anne Manier for help with the exoskeleton fabrication. Additionally, we thank all the subjects who volunteered to be part of this study. This work was supported by NIH R21 NS062119 (DPF) and F32 HD055010 (CLL).

Figures

Figure 4.1 Powered ankle exoskeleton.
Subjects wore a custom fit orthosis on their left lower limb. The orthosis was hinged at the ankle to allow free sagittal plane rotation. Soleus electromyographic (EMG) activation was recorded and processed to be used to control air pressure in the artificial pneumatic muscles proportionally. As air pressure increased, the artificial muscles started to develop tension and become shortened, allowing the powered exoskeleton to provide plantar flexor torque controlled by soleus muscle activation.

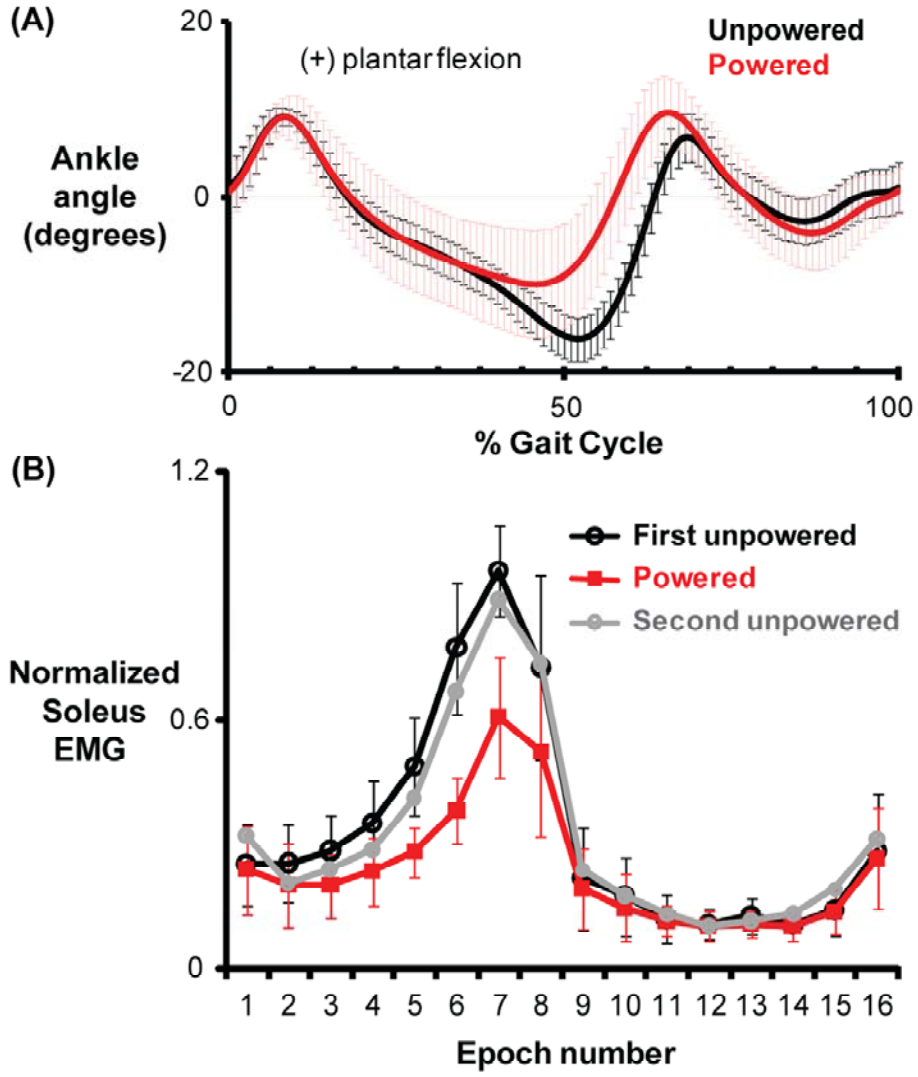

Figure 4.2 Ankle joint angle profile (A) and normalized soleus EMG (B). Data are the average of all subjects. (A) Ankle joint angle profiles are shown for unpowered (black) and powered condition (red). The error bars represent ± 1 standard deviation. Positive values indicate ankle plantar flexion. Ankle joint angle profiles during powered walking started to deviate from the ankle angle profiles of unpowered walking at epoch 7 and had greater plantar flexion during late stance. (B) Normalized soleus EMG of each time epoch was shown for the first unpowered (black), powered (red), and second unpowered (grey). The mean EMG values of each epoch were normalized to the largest value of the first unpowered condition. During powered walking, subjects had lower soleus EMG activation during mid-to-late stance.

Figure 4.3 Normalized H-wave amplitude (A), normalized soleus EMG amplitude (B), and normalized ratio of H-wave amplitude to background EMG (C).
Amplitudes of H-wave and soleus rectified EMG were first normalized to the peak-to-peak amplitude of M_{max} of that time epoch. To reduce the inter-subject variability, we then normalized the amplitudes in each condition to the values of the first unpowered condition. Thus, soleus EMG amplitude and H-reflex measurements in the first unpowered condition were 1 (100%) for the three epochs. (A) Normalized H-wave amplitudes. Subjects had significantly lower H-wave amplitudes at epoch 5 (0.76±0.13, p=0.0035) and 6 (0.80±0.22, p=0.0059) but epoch 8 (0.88±0.46, p=0.51) during powered walking. (B) Normalized soleus EMG amplitude. Subjects had significantly lower soleus EMG activation during the powered condition (epoch 5: 0.60±0.17, epoch 6: 0.52±0.20, epoch 8: 0.73±0.22). (C) Normalized ratio of H-wave amplitude to background EMG. We also normalized the ratio between H-wave amplitude and background EMG in each condition to the ratio of first unpowered condition. The ratio of the three time epochs during powered walking were slightly greater (p>0.05) compared to the unpowered conditions.

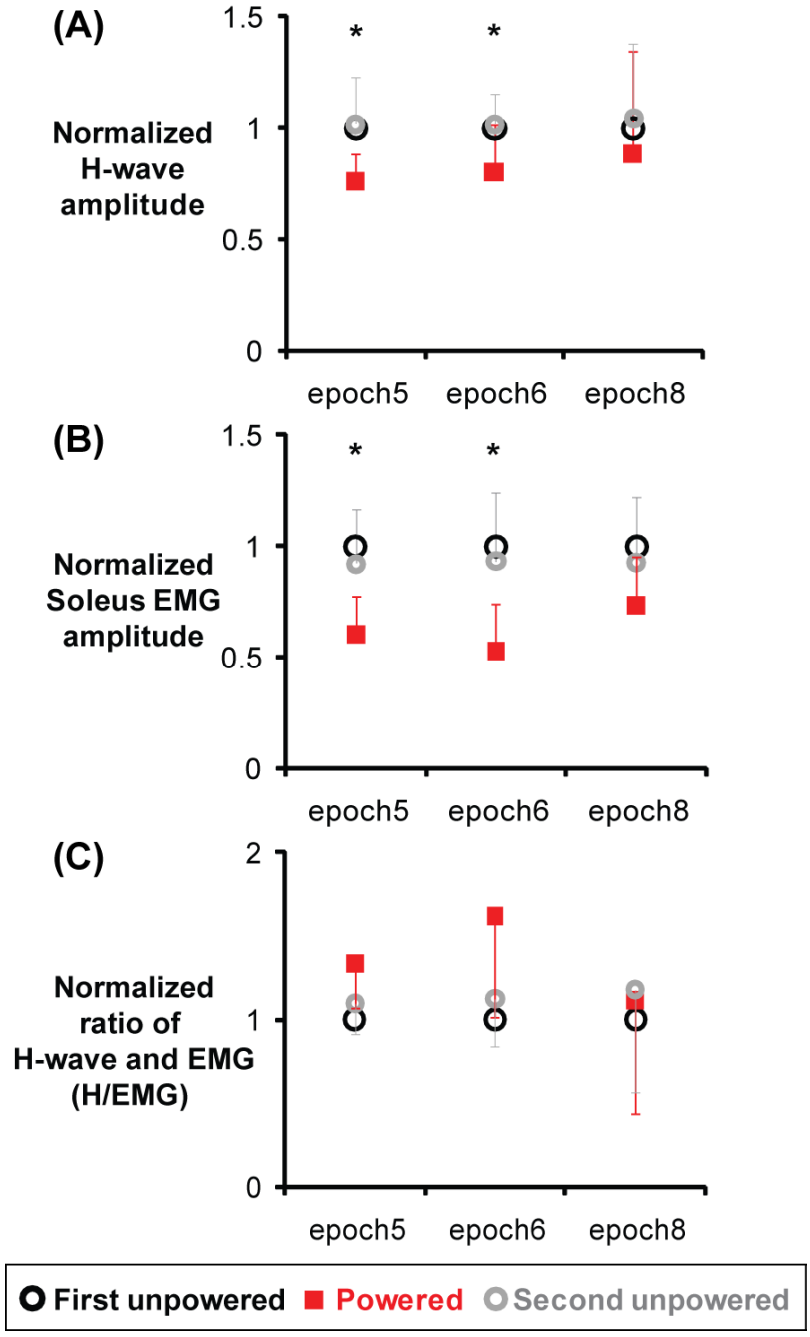
(A)
Normalized H-wave amplitude
1.5
1
0.5
0
*
*
epoch5
epoch6
epoch8
(B)
Normalized Soleus EMG amplitude
1.5
1
0.5
0
*
*
epoch5
epoch6
epoch8
(C)
Normalized ratio of H-wave and EMG (H/EMG)
2
1
0
epoch5
epoch6
epoch8
First unpowered
Powered
Second unpowered

References

af Klint R, Nielsen JB, Cole J, Sinkjaer T, Grey MJ (2008) Within-step modulation of leg muscle activity by afferent feedback in human walking. Journal of Physiology-London 586: 4643-4648

af Klint R, Nielsen JB, Sinkjaer T, Grey MJ (2009) Sudden Drop in Ground Support Produces Force-Related Unload Response in Human Overground Walking. Journal of Neurophysiology 101: 1705-1712

Aoyagi D, Ichinose WE, Harkema SJ, Reinkensmeyer DJ, Bobrow JE (2007) A robot and control algorithm that can synchronously assist in naturalistic motion during body-weight-supported gait training following neurologic injury. In: 10th IEEE International Conference on Rehabilitation Robotics, Noordwijk, NETHERLANDS, pp 387-400

Banala SK, Kim SH, Agrawal SK, Scholz JP (2007) Robot Assisted Gait Training With Active Leg Exoskeleton (ALEX). In: 10th IEEE International Conference on Rehabilitation Robotics, Noordwijk, NETHERLANDS, pp 2-8

Bastian AJ (2008) Understanding sensorimotor adaptation and learning for rehabilitation. Current Opinion in Neurology 21: 628-633

Cain SM, Gordon KE, Ferris DP (2007) Locomotor adaptation to a powered ankle-foot orthosis depends on control method. Journal of Neuroengineering and Rehabilitation 4

Capaday C (1997) Neurophysiological methods for studies of the motor system in freely moving human subjects. J Neurosci Methods 74: 201-218

Capaday C, Stein RB (1986) Amplitude modulation of the soleus H-reflex in the human during walking and standing. Journal of Neuroscience 6: 1308-1313

Capaday C, Stein RB (1987) Difference in the amplitude of the human soleus H reflex during walking and running. Journal of Physiology (London) 392: 513-522

Chen Y, Chen XY, Jakeman LB, Chen L, Stokes BT, Wolpaw JR (2006) Operant conditioning of H-reflex can correct a locomotor abnormality after spinal cord injury in rats. Journal of Neuroscience 26: 12537-12543

Colombo G, Wirz M, Dietz V (2001) Driven gait orthosis for improvement of locomotor training in paraplegic patients. Spinal Cord 39: 252-255

Crespo LM, Reinkensmeyer DJ (In press) Review of control strategies for robotic movement training after neurologic injury. Journal of Neuroengineering and Rehabilitation

Dietz V (2001) Spinal cord lesion: effects of and perspectives for treatment. Neural Plast 8: 83-90.

Dietz V (2002) Proprioception and locomotor disorders. Nature Reviews Neuroscience 3: 781-790

Dyhre-Poulsen P, Simonsen EB (2001) H reflexes recorded during locomotion. In: Gandevia SC, Proske U, Stuart DG (eds) Conference on Neural Mechanisms of Sensorimotor Control, Cairns, Australia, pp 377-383

Dyhre-Poulsen P, Simonsen EB, Voigt M (1991) Dynamic control of muscle stiffness and H reflex modulation during hopping and jumping in man. Journal of Physiology (London) 437: 287-304

Edgerton VR, Roy RR (2009) Robotic training and spinal cord plasticity. Brain Research Bulletin 78: 4-12

Emken JL, Benitez R, Reinkensmeyer DJ (2007) Human-robot cooperative movement training: Learning a novel sensory motor transformation during walking with robotic assistance-as-needed. Journal of Neuroengineering and Rehabilitation 4

Emken JL, Harkema SJ, Beres-Jones JA, Ferreira CK, Reinkensmeyer DJ (2008) Feasibility of manual teach-and-replay and continuous impedance shaping for robotic locomotor training following spinal cord injury. Ieee Transactions on Biomedical Engineering 55: 322-334

Ferris DP, Aagaard P, Simonsen EB, Farley CT, Dyhre-Poulsen P (2001) Soleus H-reflex gain in humans walking and running under simulated reduced gravity. Journal of Physiology (London) 530: 167-180

Ferris DP, Czerniecki JM, Hannaford B (2005) An ankle-foot orthosis powered by artificial pneumatic muscles. Journal of Applied Biomechanics 21: 189-197

Ferris DP, Gordon KE, Sawicki GS, Peethambaran A (2006) An improved powered ankle-foot orthosis using proportional myoelectric control. Gait and Posture 23: 425-428

Ferris DP, Kinnaird CR (2008) Robotic lower limb orthoses for gait rehabilitation after incomplete spinal cord injury. In: Proceedings of the 2008 Annual Meeting of the American Spinal Injury Association, June 19-22, 2008, San Diego, CA.

Gordon KE, Ferris DP (2007) Learning to walk with a robotic ankle exoskeleton. Journal of Biomechanics 40: 2636-2644

Gordon KE, Sawicki GS, Ferris DP (2006) Mechanical performance of artificial pneumatic muscles to power an ankle-foot orthosis. Journal of Biomechanics 39: 1832-1841

Hess F, van Hedel HJA, Dietz V (2003) Obstacle avoidance during human walking: H-reflex modulation during motor learning. Experimental Brain Research 151: 82-89

Huang VS, Krakauer JW (2009) Robotic neurorehabilitation: a computational motor learning perspective. Journal of Neuroengineering and Rehabilitation 6

Knikou M (2008) The H-reflex as a probe: Pathways and pitfalls. Journal of Neuroscience Methods 171: 1-12

Luft AR, Buitrago MM (2005) Stages of motor skill learning. Molecular Neurobiology 32: 205-216

Mazzaro N, Grey MJ, Sinkjaer T (2005a) Contribution of afferent feedback to the soleus muscle activity during human locomotion. Journal of Neurophysiology 93: 167-177

Mazzaro N, Grey MJ, Sinkjaer T, Andersen JB, Pareyson D, Schieppati M (2005b) Lack of on-going adaptations in the soleus muscle activity during

walking in patients affected by large-fiber neuropathy. Journal of Neurophysiology 93: 3075-3085
Mazzocchio R, Kitago T, Liuzzi G, Wolpaw JR, Cohen LG (2006) Plastic changes in the human H-reflex pathway at rest following skillful cycling training. Clinical Neurophysiology 117: 1682-1691
Mynark RG, Koceja DM (2002) Down training of the elderly soleus H reflex with the use of a spinally induced balance perturbation. Journal of Applied Physiology 93: 127-133
Nielsen JB, Sinkjaer T (2002) Afferent feedback in the control of human gait. Journal of Electromyography and Kinesiology 12: 213-217
Phadke CP, Wu SS, Thompson FJ, Behrman AL (2007) Comparison of soleus H-reflex modulation after incomplete spinal cord injury in 2 walking environments: Treadmill with body weight support and overground. Archives Of Physical Medicine And Rehabilitation 88: 1606-1613
Reinkensmeyer DJ, Patton JL (2009) Can Robots Help the Learning of Skilled Actions? Exercise and Sport Sciences Reviews 37: 43-51
Romano C, Schieppati M (1987) Reflex excitability of human soleus motoneurones during voluntary shortening or lengthening contractions. J Physiol (Lond) 390: 271-284
Rossignol S, Dubuc RJ, Gossard JP (2006) Dynamic sensorimotor interactions in locomotion. Physiological Reviews 86: 89-154
Sawicki GS, Domingo A, Ferris DP (2006) The effects of powered ankle-foot orthoses on joint kinematics and muscle activation during walking in individuals with incomplete spinal cord injury. Journal of Neuroengineering and Rehabilitation 3: 3
Schneider C, Capaday C (2003) Progressive adaptation of the soleus H-reflex with daily training at walking backward. Journal of Neurophysiology 89: 648-656
Schneider C, Lavoie BA, Capaday C (2000) On the origin of the soleus H-reflex modulation pattern during human walking and its task-dependent differences. J Neurophysiol 83: 2881-2890.
Shefchyk SJ, Jordan LM (1985) Excitatory and Inhibitory Postsynaptic Potentials in Alpha-Motoneurons Produced During Fictive Locomotion by Stimulation of the Mesencephalic Locomotor Region. Journal of Neurophysiology 53: 1345-1355
Simonsen EB, Dyhre-Poulsen P (1999) Amplitude of the human soleus H reflex during walking and running. Journal of Physiology-London 515: 929-939
Sinkjaer T (1997) Muscle, reflex and central components in the control of the ankle joint in healthy and spastic man. Acta Neurol Scand Suppl 170: 1-28
Sinkjaer T, Andersen JB, Larsen B (1996) Soleus stretch reflex modulation during gait in humans. Journal of Neurophysiology 76: 1112-1120
Stein RB, Capaday C (1988) The modulation of human reflexes during functional motor tasks. Trends in Neurosciences 11: 328-332
Trimble MH, Behrman AL, Flynn SM, Thigpen MT, Thompson FJ (2001) Acute effects of locomotor training on overground walking speed and H-reflex

modulation in individuals with incomplete spinal cord injury. Journal of Spinal Cord Medicine 24: 74-80

Trimble MH, Koceja DM (1994) Modulation of the triceps surae H-reflex with training. International Journal of Neuroscience 76: 293-303

Trimble MH, Kukulka CG, Behrman AL (1998) The effect of treadmill gait training on low-frequency depression of the soleus H-reflex: comparison of a spinal cord injured man to normal subjects. Neuroscience Letters 246: 186-188

Ung RV, Imbeault MA, Ethier C, Brizzi L, Capaday C (2005) On the potential role of the corticospinal tract in the control and progressive adaptation of the soleus h-reflex during backward walking. Journal of Neurophysiology 94: 1133-1142

Werner C, Von Frankenberg S, Treig T, Konrad M, Hesse S (2002) Treadmill training with partial body weight support and an electromechanical gait trainer for restoration of gait in subacute stroke patients: a randomized crossover study. Stroke 33: 2895-2901

Wirz M, Colombo G, Dietz V (2001) Long term effects of locomotor training in spinal humans. Journal of Neurology Neurosurgery and Psychiatry 71: 93-96

Wolpaw JR (1997) The complex structure of a simple memory. Trends in Neurosciences 20: 588-594

Wolpaw JR, Okeefe JA (1984) Adaptive Plasticity in the Primate Spinal Stretch Reflex - Evidence for a 2-Phase Process. Journal of Neuroscience 4: 2718-2724

Yang JF, Fung J, Edamura M, Blunt R, Stein RB, Barbeau H (1991a) H-reflex modulation during walking in spastic paretic subjects. Canadian Journal of Neurological Sciences 18: 443-452

Yang JF, Stein RB, James KB (1991b) Contribution of peripheral afferents to the activation of the soleus muscle during walking in humans. Experimental Brain Research 87: 679-687

Chapter V

Joint kinetic response during unexpectedly reduced plantar flexor torque provided by a robotic ankle exoskeleton during walking

Abstract

During human walking, plantar flexor activation in late stance helps to generate a stable and economical gait pattern. Because plantar flexor activation is highly mediated by proprioceptive feedback, the nervous system must modulate reflex pathways to meet the mechanical requirements of gait. The purpose of this study was to quantify the mechanical output of the plantar flexor reflex response during a novel unexpected gait perturbation. We used a robotic ankle exoskeleton to mechanically amplify the ankle torque output resulting from soleus muscle activation. We recorded lower-body kinematics, ground reaction forces, and electromyography during steady state walking and during randomly perturbed steps when the exoskeleton assistance was unexpectedly turned off. We also measured soleus Hoffmann (H-) reflexes at late stance during the two conditions. Subjects reacted to the unexpectedly decreased exoskeleton assistance by greatly increasing soleus muscle activity about 60 milliseconds after the ankle angle deviated from the control condition (p<0.001). There were large differences in ankle kinematic and electromyography patterns for the

perturbed and control steps, but the total ankle moment was almost identical for the two conditions (p=0.13). The ratio of soleus H-reflex amplitude to background electromyography was not significantly different between the two conditions (p=0.4). This is the first study to show that plantar flexor reflex responses during perturbed walking are remarkably well modulated to maintain a consistent ankle joint moment pattern. Our findings are particularly useful for the development of neuromusculoskeletal computer simulations of human walking that need to adjust reflex gains appropriately for biomechanical analyses.

Key words: Gait; powered orthosis; H-reflex; locomotion; inverse dynamics; joint kinetics; EMG

Introduction

To generate a stable and economical gait pattern, it is critical to activate ankle plantar flexor muscles with the correct timing and appropriate magnitude to produce trailing limb push-off during late stance. A powered walking model by Kuo indicates that push-off performed along the trailing leg immediately before heel strike of the leading leg is four times less costly than driving the stance leg with hip mechanical power at other time points during the gait cycle (Kuo 2002). In humans, the ankle mechanical power burst provides the majority of positive work required to restore the energy lost in redirecting the center of mass in step-to-step transitions (Kuo et al. 2005). In addition to the correct timing, adequate magnitude of ankle push-off is necessary to reduce energy loss due to collision in

the leading leg. These two factors, timing and amplitude of ankle push-off, may be used to explain why many pathological gaits exhibit high metabolic costs (Sawicki et al. In press).

As plantar flexor muscle activity is largely mediated by proprioceptive feedback during walking (Yang et al. 1991; Sinkjaer et al. 1996; Nielsen and Sinkjaer 2002; Mazzaro et al. 2005a; Mazzaro et al. 2005b; Rossignol et al. 2006; af Klint et al. 2008; af Klint et al. 2009), it is important that the nervous system modulates reflex pathways to meet mechanical requirement of gait. Thus, well-modulated reflex responses play an important role in aiding in correcting gait perturbations and preventing falling by rapidly regulating motor neuron discharge (Nielsen and Sinkjaer 2002). Previous studies have shown sudden increases in ankle plantar flexor electromyographic (EMG) activation following a perturbation that rapidly dorsiflexes the ankle during walking (Yang et al. 1991; Sinkjaer et al. 1996). The stretch reflex increases ankle plantar flexor activation, augmenting the ankle plantar flexor moment and keeping the lower limb from collapsing when an external perturbation is encountered.

Mechanical quantification of reflex responses to gait perturbation is necessary to add accurate reflexes to musculoskeletal computer simulations of gait. Adding reflexes to the models allows for a more physiologically realistic simulation (Pandy 2001; Pearson et al. 2006), especially when the simulation dynamics involve responses to external perturbations. Most current musculoskeletal computer simulations of gait lack physiologically based reflex responses. They often use predetermined limb trajectories and joint kinetics from

experimental data, and/or implement optimization routines for some objective features of gait (e.g. minimizing deviation of the trunk from upright posture (Gilchrist and Winter 1997).

We have limited understanding of how reflex responses directly impact joint mechanical output during human walking. Past studies on plantar flexor reflex response to perturbations have focused on muscle activation and joint kinematics (Yang et al. 1991; Sinkjaer et al. 1996; Nielsen and Sinkjaer 2002; Mazzaro et al. 2005a; Mazzaro et al. 2005b; Rossignol et al. 2006; af Klint et al. 2008; af Klint et al. 2009). It is not clear if there is a kinetic goal for the nervous system in modulating reflex responses during gait. As muscle activation increases during a perturbation because of the reflex response, does the response maintain joint moments to a level similar to unperturbed gait?

The purpose of this study was to mechanically quantify joint kinetics of reflex responses during an unexpected gait perturbation. Previous studies on motor adaptation to a robotic ankle exoskeleton found that subjects decreased soleus EMG amplitude by 28-35% when walking with exoskeleton plantar flexor assistance (Gordon and Ferris 2007; Sawicki and Ferris 2008). It seemed likely that turning off the robotic assistance unexpectedly after adaptation would cause a gait perturbation and result in a reflex response stabilizing the body. We examined neurologically intact subjects that had trained with the robotic ankle exoskeleton. In addition to kinematics and kinetics of their reflex responses, we also recorded soleus Hoffmann (H-) reflexes at late stance.

Methods

Subjects

Eleven healthy subjects (5 male, 6 female) gave written informed consent and participated in the study. The University of Michigan Medical School Institutional Review Board approved the protocol, and the study conformed to the standards set by the Declaration of Helsinki.

Experimental design

We constructed a custom-made exoskeleton (Fig. 1) for the left lower limb of each subject. The ankle exoskeleton consisted of a carbon fiber shank section and a polypropylene foot section. A metal hinge between the sections allowed free sagittal plane rotation of the ankle joint. Two artificial pneumatic muscles attached to the posterior of the exoskeleton provided plantar flexor torque. We implemented proportional myoelectric control (i.e., amplitude and timing) of the artificial muscles through a desktop computer and real-time control board (dSPACE Inc., Wixom, MI, USA) (Ferris et al. 2006; Gordon and Ferris 2007; Kao and Ferris 2009; Kinnaird and Ferris 2009). A custom real-time computer controller regulated air pressure in the artificial plantar flexor muscles proportional to the processed soleus electromyographic signals (EMG) via a pressure regulator. EMG signal from soleus was high-pass filtered with a second-order Butterworth filter (20-Hz cutoff frequency) to remove movement artifact, full wave rectified, and low-pass filtered with a second-order Butterworth filter (10-Hz cutoff frequency) to smooth the signal. Adjustable gains scaled the control signals and a threshold cutoff eliminated background noise. We used a

footswitch (B&L Engineering, Santa Ana, CA, USA) in the left shoe to detect heel strikes and calculate average gait cycle.

Before testing the motor response to the unexpectedly reduced ankle plantar flexor torque, subjects had completed two 30-minute treadmill training sessions for walking with the powered ankle exoskeleton controlled by soleus EMG (Gordon and Ferris 2007). Subjects walked with the powered ankle assistance for at least 15 minutes (**Powered**). Then the soleus H-reflex was evoked at late stance during steady state powered walking. Finally, during random steps, the power was unexpectedly turned off at mid-stance inducing a perturbation (**Perturbed**). After recording approximately 5 steps of perturbation without the electrical stimulations, soleus H-reflex was evoked during late stance of the perturbed steps when power was unexpectedly turned off. The perturbations occurred randomly and were at least 12 seconds apart (with a range of 12 to 38 seconds).

Data acquisition and analysis

We collected lower body kinematics, artificial muscle force, electromyography (EMG) and ground reaction forces (GRFs) while subjects walked on a custom-constructed force-measuring split-belt treadmill at 1.25 m/s. The three-dimensional kinematic data were collected using an 8-camera video system (120 Hz, Motion Analysis Corporation, Santa Rosa, CA, USA). Artificial muscle force data were collected with force transducers (1200 Hz, Omega Engineering, Stamford, CT, USA) mounted on the bracket of the exoskeleton. We estimated the mechanical torque, power and work done by the exoskeleton

with the measurement of artificial muscle moment arm and ankle kinematic data. We placed bipolar surface electrodes on the left shank to record EMGs (1200 Hz, Konigsberg Instruments Inc., Pasadena, CA, USA) from tibialis anterior (TA), soleus (SOL), medial gastrocnemius (MG), and lateral gastrocnemius (LG). We used commercial software (Visual3D, C-Motion Inc., Germantown, MD, USA) to calculate joint angles as well as the joint kinetics by inverse dynamics analysis. Lower limb inertial properties were estimated based on anthropometric measurements of subjects (Zatsiorsky 2002) and adjusted to account for the added exoskeleton mass. Ankle joint work was calculated over the whole gait cycle. We also determined when the soleus EMG and ankle angle patterns during the perturbed steps started to deviate from the patterns during the unperturbed steps (mean± 1 standard deviation).

Soleus H-reflex measurements

We measured the soleus H-reflex in eight out of the eleven subjects. We elicited the soleus H-reflex by stimulating (DS7AH constant current stimulator, Digitimer Ltd., Hertfordshire, England) the tibial nerve with a cathode placed in the popliteal fossa and an anode (7-cm diameter) on the patella. The electrical stimulus was a 1-millisecond monophasic square pulse. To locate the optimal nerve stimulation site, we delivered a couple of stimuli on different spots within the popliteal fossa while subjects were standing motionless with the ankle exoskeleton unpowered. The criterion for choosing the site of cathode placement was the largest peak-to-peak amplitude of M-wave at a constant intensity of stimulation.

We recorded the soleus H-reflex during constantly powered walking (powered) and during the steps when power was unexpectedly turned off at mid-stance (perturbed). We divided the gait cycle into 16 equal epochs (~10 epochs during stance). We evoked soleus H-reflex at late stance (epoch 8) by which point the robotic ankle assistance started to diminish. Epoch 8 is also about the time when soleus activity reached to its peak amplitude. We used a custom-written program and a real-time control board (dSPACE Inc.) to control the timing of electrical stimulations and to measure the resulting M-wave and H-wave peak-to-peak amplitudes (2000 Hz).

The size of the M-wave as a percentage of the maximal M-wave (i.e., M_{max}, maximal evoked muscle response) has been regularly used to control constant effective stimulus intensity to the afferent nerve (Capaday 1997; Simonsen and Dyhre-Poulsen 1999; Ferris et al. 2001). Stimulating to produce an M-wave that is a constant percentage of M_{max} results in the recruitment of approximately the same number of motor axons, indicating that stimulus intensity to the afferent nerve is also constant (Capaday and Stein 1986). While walking, the relative movement between the stimulating electrode and the nerve may change the amplitude of the M_{max} over a stride (Simonsen and Dyhre-Poulsen 1999). To account for changes in M_{max}, we first collected 3 M-wave measurements at epoch 8 by delivering a larger stimulus than the one which evoked M_{max} during quiet standing (at least 1.2 times of stimulation intensity for evoking M_{max} during quiet standing). The stimulus intensity delivered to the tibial nerve for the H-reflex measurements was the intensity which evoked a

corresponding M-wave that was 25% of M_{max} for epoch 8. The program monitored the peak-to-peak amplitude of the M-wave produced by the stimulus, and calculated the ratio of the M-wave amplitude to the M_{max} for epoch 8. We only accepted H-reflex measurements where the M-wave was 25 ± 10% of the M_{max} at epoch 8. To ensure constant stimulus intensity, we manually adjusted the intensity of subsequent stimuli if the ratio was not within the acceptable range. We collected 10 measurements of H-reflex where the corresponding M-wave was 25 ± 10% of M_{max} in epoch 8.

Since the H-reflex amplitude depends on the background level of motor activity (Capaday and Stein 1987; Capaday 1997), we calculated the ratio of H-reflex amplitude to its corresponding background EMG amplitude. The background activity of the soleus EMG was estimated from the mean value of the rectified averaged soleus EMG during the second half of epoch 7 (~70 ms before the tibial nerve stimulus with duration of 35 ms).

Statistics

We performed multiple paired t-tests to detect differences in the primary variables between the two conditions (powered versus perturbed). The primary variables were ankle positive and negative work, peak ankle moment, ankle angle at late stance, the second peak of overall support moment and of vertical GRF in the trailing leg, the first peak of vertical GRF in the contralateral leading leg, and the ratio of soleus H-reflex amplitude to the background EMG. We set the significance level at $p<0.05$ and used Bonferroni correction. All statistical

analyses were performed in JMP statistical software (SAS institute Inc., Cary, NC, USA).

Results

Subjects reacted to the unexpectedly decreased exoskeleton plantar flexor assistance by increasing soleus muscle activation within the perturbed step to recover from the perturbation. During steady-state powered walking, the ankle exoskeleton provided a substantial plantar flexor moment (0.77±0.26 Nm/kg, mean±SD) that was ~50% of the net ankle plantar flexor moment during push-off (1.50±0.12 Nm/kg) (Fig 2a). When exoskeleton power was turned off unexpectedly, subjects reacted quickly by increasing soleus (Fig 2b) and other shank muscle activation (Fig 3) for the second half of stance. The soleus EMG pattern during perturbed steps deviated from the soleus EMG pattern during powered steps (mean + 1SD) with a time lag of 60±29 (mean±SD) milliseconds after the ankle angle deviated from the pattern of powered steps. The majority of subjects had a time lag of less than 60 ms. Only two out of the eleven subjects had a longer time lag (90 and 133 ms, individually).

The ankle moment pattern during the perturbed steps was remarkably similar to the ankle moment pattern during unperturbed steps (Fig 2e) as a result of rapid increase in soleus EMG (peak plantar flexor moment; perturbed: 1.43±0.09 Nm/kg; powered: 1.50±0.12 Nm/kg; t-test, p=0.13). There were noticeable differences in the ankle joint angle (Fig 2c), ankle joint velocity (Fig 2d), and ankle power (Fig 2f) profiles during the perturbed versus powered steps.

During perturbed steps, subjects had a more dorsiflexed ankle posture by ~8 degrees (peak dorsiflexion; perturbed: -16.64°±5.09°; powered: -8.35°±6.75°; p<0.0001), greater angular velocity towards dorsiflexion at late stance, and smaller ankle plantar flexion at toe-off by ~8 degrees (peak plantar flexion; perturbed: 3.75°±6.29°; powered: 11.66°±4.21°, p<0.0001). Due to the differences in ankle kinematics (Fig 2c, 2d), subjects had different ankle power profiles between powered and perturbed steps. Subjects had significantly smaller ankle positive work (mean±SD; perturbed: 14.6±3.4 J; powered: 24.5±3.4 J; p<0.0001) and greater negative work (perturbed: -17.4±4.7 J; powered: -8.3±3.6 J; p<0.0001) during the perturbed steps.

When ankle exoskeleton assistance was reduced during the random perturbed steps, subjects demonstrated notably different overall support moment profiles along with an increased knee extensor moment and delayed hip flexor moment (Fig 4). The second peak of the overall support moment was ~36% more for the perturbed steps compared to the powered steps (perturbed: 1.00±0.24 Nm/kg; powered: 0.64±0.26 Nm/kg; p<0.0001). Correspondingly, during the perturbed steps, subjects had greater knee power absorption (perturbed: -1.77±0.52 W/kg; powered: -0.84±0.19) due to a more flexed knee posture at late stance. Although subjects walked with similar hip joint angle profiles, the delayed hip flexor moment during perturbed steps resulted in a delayed but increased hip flexion velocity and thus, an increase in hip joint power generation following the perturbation (perturbed: 1.09±0.48; powered: 0.70±0.12).

Despite the similarity in the ankle moment magnitude, there were differences in vertical ground reaction forces (GRFs) between conditions. The second peak of the vertical ground reaction force in the trailing leg was ~11% less for the perturbed steps compared to the powered steps (perturbed: 9.93±0.71 N/kg; powered: 11.13±0.88 N/kg; p=0.0003) (Fig 4). The first peak of the vertical ground reaction force in the contralateral leading leg was ~15% greater following the perturbed steps compared to following the powered steps (perturbed: 12.53±0.97 N/kg; powered: 10.93±0.43 N/kg; p<0.0001).

H-reflex amplitude

Subjects had slightly higher H-reflex amplitude during the perturbed steps than during the control steps (perturbed: 28.3±18.8% of M_{max}; powered: 21.8±16.2% of M_{max}; p=0.117). However, background soleus EMG was also higher for the perturbed steps compared to the powered steps (perturbed: 1.6±0.7% of M_{max}; powered: 1.0±0.2% of M_{max}; p=0.055). As a result, when normalizing H-reflex to the background soleus EMG, there was no significant difference between conditions (perturbed: 26.21±22.29; powered: 23.06±19.67; p=0.404).

Discussion

When encountering an unexpected decrease in mechanical assistance from a powered ankle exoskeleton at mid-stance, subjects reacted quickly by rapidly increasing soleus muscle activation. Compared to the unperturbed steps, subjects had similar soleus H-reflex amplitude in proportion to the soleus

background EMG during the perturbed steps. This indicates that the perturbation did not alter the reflex gain away from what was normally set during steady state walking.

The rapid response to the perturbation produced an ankle joint moment profile that was almost identical to the unperturbed control condition. However, there was a different overall support moment pattern due to a greater knee extensor moment and delayed hip flexor moment. Thus, contrary to past studies (Winter 1980; Winter 1989), the overall support moment pattern may not be as invariant during human gait as suggested. Our results are the first to demonstrate that the nervous system sets reflex gain during human walking to produce invariant ankle joint moment patterns in the event of a gait perturbation. While we only examined a single type of perturbation (i.e. increased dorsiflexion), the general principle of an invariant ankle joint moment pattern may hold true for other perturbations as well.

A limitation of our study is that our protocol required that subjects undergo multiple perturbations and thus, could have demonstrated accommodation to the perturbation. Each subject underwent approximately thirty-five perturbations. Five of these were for measuring kinematics, kinetics, and EMG only, and thirty of these were for H-reflex measurements. When comparing mean responses of the non-H-reflex trials, we found no evidence for attenuation of the reflex response. That is, the first response was almost identical to the mean response for all the non-H-reflex trials.

The decrease in ankle work by the trailing limb resulted in a significantly greater collision in the contralateral leading leg. This finding supports the predictions of simple walking models that ankle push-off during human walking is a critical factor in generating an efficient gait. The powered walking model by Kuo (2002) demonstrated an increased energy lost at heel strike in the leading leg when decreasing ankle push-off energy input to the trailing leg (Kuo 2002). Moreover, when the amount of collision exceeds the amount of ankle push-off, additional positive work must be then performed during single support to maintain a steady walking speed (Kuo et al. 2005). This additional positive work may be performed by active hip torque and is very costly (Kuo 2002). Individuals with pathological gaits usually demonstrate insufficient muscle strength and low ankle plantar flexor muscle activation (Nadeau et al. 1999; Chen et al. 2005; Den Otter et al. 2007; Lamontagne et al. 2007; Turns et al. 2007; Chen and Patten 2008). To improve walking efficiency, training individuals with pathological gaits to increase push-off from the trailing limb could greatly improve their walking energetics (Sawicki et al. In press).

While there have been numerous computer simulations of musculoskeletal models for human walking, few have included reflexes or the ability to respond to perturbations. Computer simulations are a powerful tool to increase our understanding of neural and biomechanical mechanisms involved in human locomotion. Implementing components of reflex responses to simulation models is particularly useful for identifying the specific roles of sensory feedback in regulating muscle activity (Ekeberg and Pearson 2005; Pearson et al. 2006).

However, most model simulations have focused on steady state locomotion. To adequately model human movement during situations that could cause musculoskeletal injury, it is important to adequately include reflex dynamics in the simulations.

As one example, Jo (2007) successfully implemented reflexes involved in controlling leg swing trajectory during a perturbation. The result was a fairly accurate kinematic response (Jo 2007). When encountering a gait perturbation during stance, kinetic information is likely to be more helpful in faithfully reproducing body dynamics during the perturbation. Our results demonstrated that the nervous system modulates reflex responses to maintain a consistent joint moment pattern in the event of ankle joint perturbations. Implementing a similar type of reflex scaling in neuromusculoskeletal computer simulation models could help to improve the fidelity of the simulations for studying a wider range of movement dynamics. If future experiments also document a prioritization of joint moment profiles in response to other perturbations, a general reflex scaling principle could be used for the simulations.

Conclusion

This is the first study to show that the nervous system modulates reflex responses during human walking to maintain invariant ankle joint patterns relative to unperturbed gait. Our findings suggest that ankle joint moment patterns are maintained even when the overall support moment pattern changes during a gait perturbation. This may represent a general principle governing

reflex responses to mechanical perturbations and could be easily implemented in computer simulations of neuromusculoskeletal models.

Acknowledgments

The authors thank Danielle Sandella, Kristin Carroll, Evelyn Anaka, and members of the Human Neuromechanics Laboratory for assistance in collecting data. We also thank Anne Manier for help with fabricating the exoskeleton. This work was supported by NIH R21 NS062119 (DPF) and F32 HD055010 (CLL).

Figures

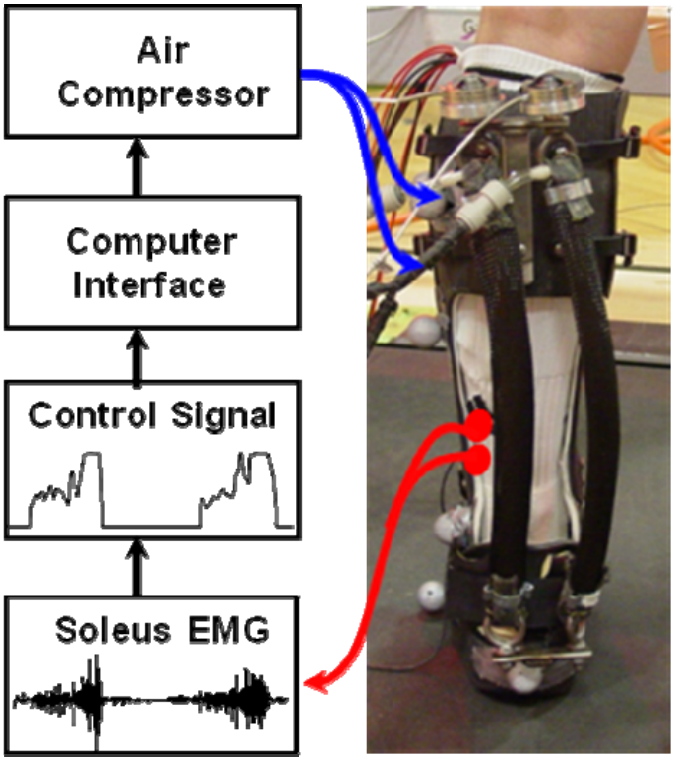

Figure 5.1 Powered ankle exoskeleton.
Subjects wore a custom fit exoskeleton on their left lower limb. The exoskeleton was hinged at the ankle to allow free sagittal plane rotation. The exoskeleton had an average weight of 1.08±0.09 kg (mean±SD) and moment arm length of 11.0±1.2 cm that varied and depended on the size of the subject. Electrical signals (EMG) of soleus activation were recorded and processed to be used to control air pressure in the artificial pneumatic muscles proportionally. As air pressure increased, the artificial muscles started to develop tension and become shortened, allowing the powered exoskeleton to provide plantar flexor torque controlled by soleus muscle activation.

Figure 5.2 Ankle joint kinematics and kinetics during constantly powered versus perturbed conditions.
Ankle profiles are shown for the powered (red dashed line, mean ± 1 SD) and perturbed steps (black line). The vertical lines represent the toe-off. Positive values indicate plantar flexion. Data are the average of all subjects. The time lag between the deviated ankle angle pattern and increased soleus EMG during the perturbed steps was determined for each subject, individually. When the control signals was turned off at midstance, the mechanical torque provided by the ankle exoskeleton was reduced largely for the rest of the stance (a). The unexpectedly reduction in the ankle exoskeleton assistance resulted in a more dorsiflexed ankle posture (c), greater angular velocity towards dorsiflexion (d), and quickly increased soleus EMG activation (b). As a result of quick increase in soleus EMG, subjects had similar ankle moment profiles (e). Thus, due to the differences in ankle kinematics, subjects had greater power absorption and less power generation during the perturbed steps (f).

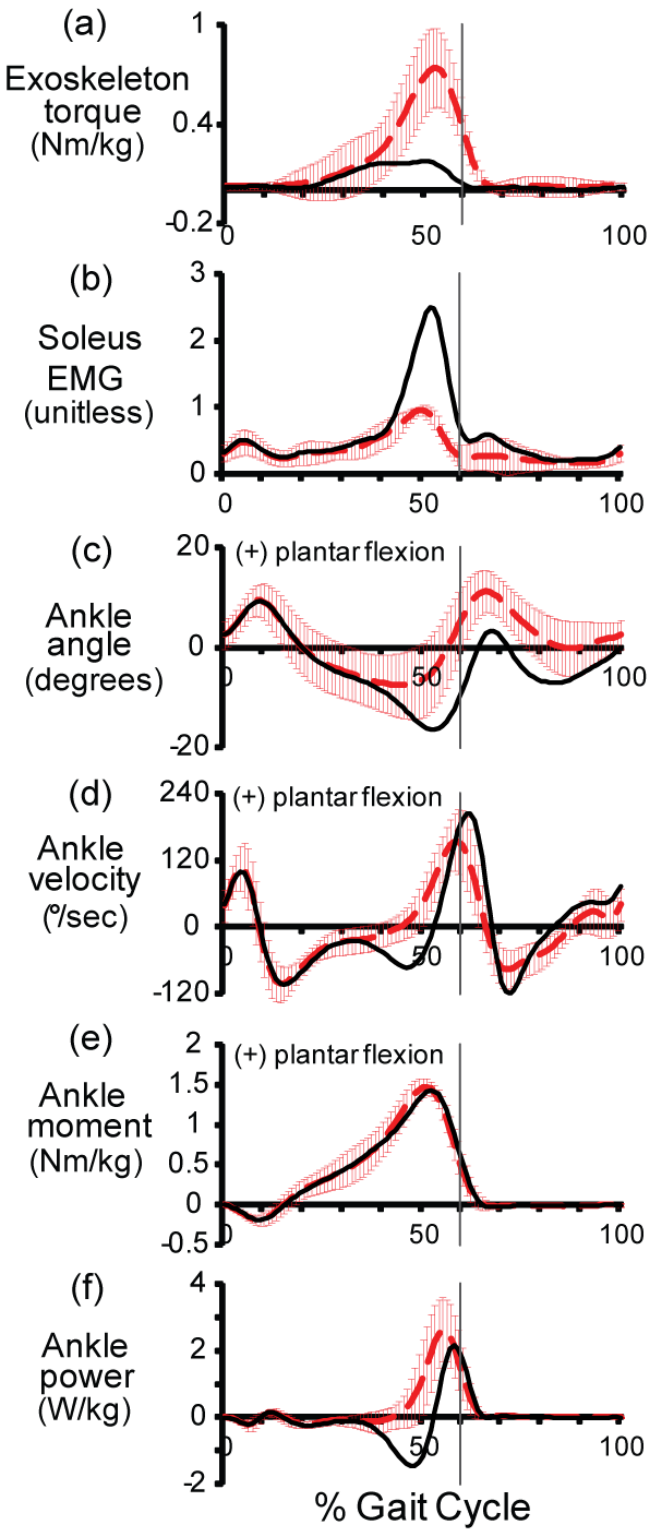
(a)
Exoskeleton torque (Nm/kg)
1
0.4
-0.2
0
50
100
(b)
Soleus EMG (unitless)
3
2
1
0
0
50
100
(c)
Ankle angle (degrees)
20
0
-20
(+) plantar flexion
0
50
100
(d)
Ankle velocity (°/sec)
240
120
0
-120
(+) plantar flexion
0
50
100
(e)
Ankle moment (Nm/kg)
2
1.5
1
0.5
0
-0.5
(+) plantar flexion
0
50
100
(f)
Ankle power (W/kg)
4
2
0
-2
0
50
100
% Gait Cycle

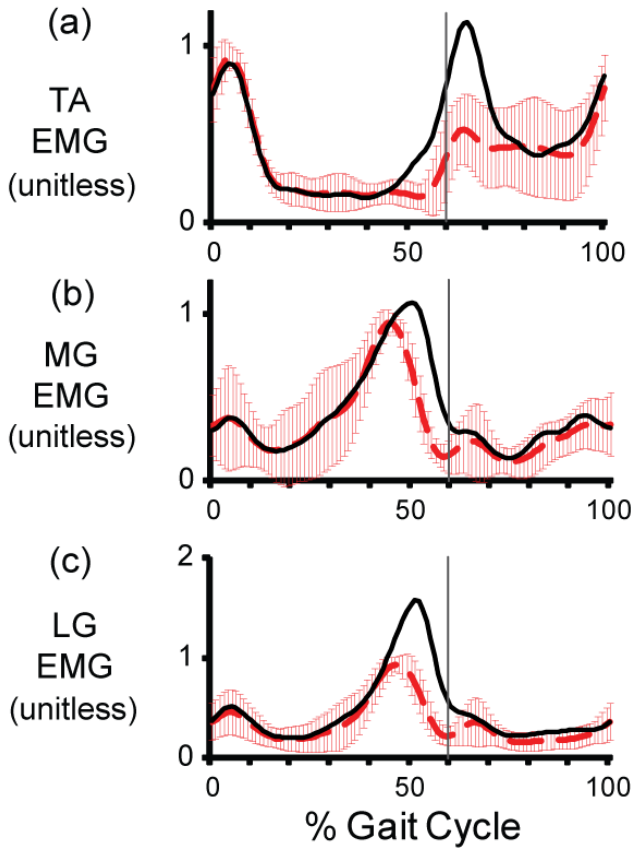

Figure 5.3 Other shank muscle activation patterns.
Tibialis anterior (TA), medial gastrocnemius (MG) and lateral gastrocnemius (LG) EMG profiles during powered (red dashed line, mean ± 1 SD) and perturbed steps (black line). Data were averaged for all subjects. All muscles were increased in amplitude following the perturbation.

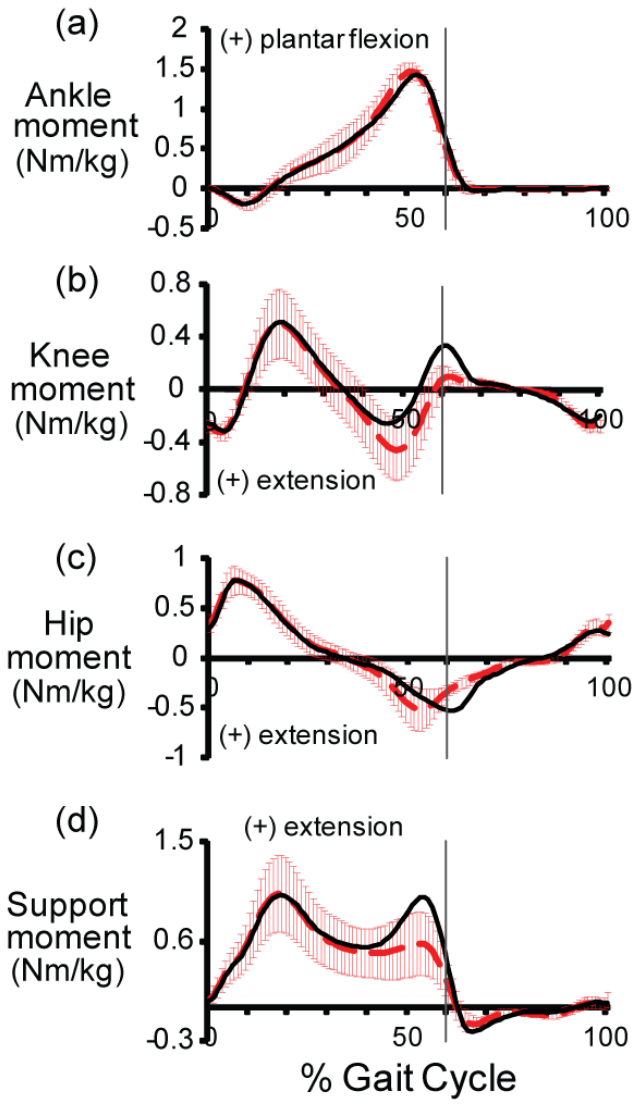

Figure 5.4 Joint moments and overall support moment during powered (red dashed line, mean ± 1 SD) and perturbed steps (black line).
The overall support moment (d) is the sum of extensor moments from hip (c), knee (b) and ankle (a) joints during stance. During perturbed steps, subjects had significantly different overall support moment at push-off with similar ankle plantar flexor moment, greater knee extensor moment and delayed hip flexor moment.

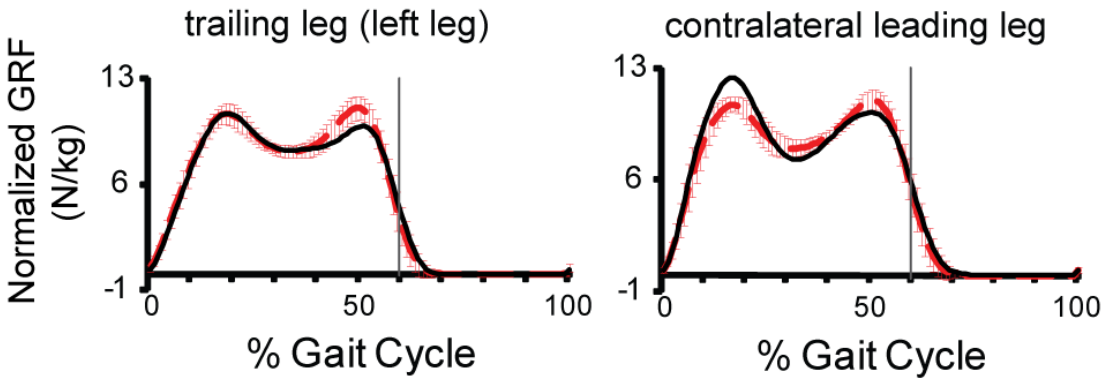

Figure 5.5 Vertical ground reaction forces (GRFs) of trailing leg and the contralateral leading leg during the powered (red dashed line, mean ± 1 SD) and perturbed steps (black line).
When the mechanical assistance was turned off at the midstance (i.e., perturbed steps), the second peak of vertical GRF in the trailing leg was reduced by ~11%.The first peak of vertical GRF in the contralateral leading leg was increased by ~15% following the perturbed steps compared to following the constantly powered steps.

References

af Klint R, Nielsen JB, Cole J, Sinkjaer T, Grey MJ (2008) Within-step modulation of leg muscle activity by afferent feedback in human walking. Journal of Physiology-London 586: 4643-4648

af Klint R, Nielsen JB, Sinkjaer T, Grey MJ (2009) Sudden Drop in Ground Support Produces Force-Related Unload Response in Human Overground Walking. Journal of Neurophysiology 101: 1705-1712

Capaday C (1997) Neurophysiological methods for studies of the motor system in freely moving human subjects. J Neurosci Methods 74: 201-218

Capaday C, Stein RB (1986) Amplitude modulation of the soleus H-reflex in the human during walking and standing. Journal of Neuroscience 6: 1308-1313

Capaday C, Stein RB (1987) Difference in the amplitude of the human soleus H reflex during walking and running. Journal of Physiology (London) 392: 513-522

Chen G, Patten C (2008) Joint moment work during the stance-to-swing transition in hemiparetic subjects. Journal of Biomechanics 41: 877-883

Chen G, Patten C, Kothari DH, Zajac FE (2005) Gait differences between individuals with post-stroke hemiparesis and non-disabled controls at matched speeds. Gait & Posture 22: 51-56

Den Otter AR, Geurts ACH, Mulder T, Duysens J (2007) Abnormalities in the temporal patterning of lower extremity muscle activity in hemiparetic gait. Gait & Posture 25: 342-352

Ekeberg O, Pearson K (2005) Computer simulation of stepping in the hind legs of the cat: An examination of mechanisms regulating the stance-to-swing transition. Journal of Neurophysiology 94: 4256-4268

Ferris DP, Aagaard P, Simonsen EB, Farley CT, Dyhre-Poulsen P (2001) Soleus H-reflex gain in humans walking and running under simulated reduced gravity. Journal of Physiology (London) 530: 167-180

Ferris DP, Gordon KE, Sawicki GS, Peethambaran A (2006) An improved powered ankle-foot orthosis using proportional myoelectric control. Gait and Posture 23: 425-428

Gilchrist LA, Winter DA (1997) A multisegment computer simulation of normal human gait. IEEE Trans Rehabil Eng 5: 290-299.

Gordon KE, Ferris DP (2007) Learning to walk with a robotic ankle exoskeleton. Journal of Biomechanics 40: 2636-2644

Jo S (2007) A neurobiological model of the recovery strategies from perturbed walking. Biosystems 90: 750-768

Kao PC, Ferris DP (2009) Motor adaptation during dorsiflexion-assisted walking with a powered orthosis. Gait and Posture 29: 230-236

Kinnaird CR, Ferris DP (2009) Medial gastrocnemius myoelectric control of a robotic ankle exoskeleton for human walking. IEEE Transactions on Neural Systems and Rehabilitation Engineering 17: 31-37

Kuo AD (2002) Energetics of actively powered locomotion using the simplest walking model. Journal of Biomechanical Engineering 124: 113-120

Kuo AD, Donelan JM, Ruina A (2005) Energetic consequences of walking like an inverted pendulum: step-to-step transitions. Exercise and Sport Sciences Reviews 33: 88-97

Lamontagne A, Stephenson JL, Fung J (2007) Physiological evaluation of gait disturbances post stroke. Clinical Neurophysiology 118: 717-729

Mazzaro N, Grey MJ, Sinkjaer T (2005a) Contribution of afferent feedback to the soleus muscle activity during human locomotion. Journal of Neurophysiology 93: 167-177

Mazzaro N, Grey MJ, Sinkjaer T, Andersen JB, Pareyson D, Schieppati M (2005b) Lack of on-going adaptations in the soleus muscle activity during walking in patients affected by large-fiber neuropathy. Journal of Neurophysiology 93: 3075-3085

Nadeau S, Gravel D, Arsenault AB, Bourbonnais D (1999) Plantarflexor weakness as a limiting factor of gait speed in stroke subjects and the compensating role of hip flexors. Clinical Biomechanics 14: 125-135

Nielsen JB, Sinkjaer T (2002) Afferent feedback in the control of human gait. Journal of Electromyography and Kinesiology 12: 213-217

Pandy MG (2001) Computer modeling and simulation of human movement. Annual Review of Biomedical Engineering 3: 245-273

Pearson K, Ekeberg O, Buschges A (2006) Assessing sensory function in locomotor systems using neuro-mechanical simulations. Trends Neurosci 29: 625-631

Rossignol S, Dubuc RJ, Gossard JP (2006) Dynamic sensorimotor interactions in locomotion. Physiological Reviews 86: 89-154

Sawicki GS, Ferris DP (2008) Mechanics and energetics of level walking with powered ankle exoskeletons. Journal of Experimental Biology 211: 1402-1413

Sawicki GS, Lewis CL, DP F (In press) It pays to have a spring in your step. Exercise and Sport Sciences Reviews

Simonsen EB, Dyhre-Poulsen P (1999) Amplitude of the human soleus H reflex during walking and running. Journal of Physiology-London 515: 929-939

Sinkjaer T, Andersen JB, Larsen B (1996) Soleus stretch reflex modulation during gait in humans. Journal of Neurophysiology 76: 1112-1120

Turns LJ, Neptune RR, Kautz SA (2007) Relationships between muscle activity and anteroposterior ground reaction forces in hemiparetic walking. Archives of Physical Medicine and Rehabilitation 88: 1127-1135

Winter DA (1980) Overall principle of lower limb support during stance phase of gait. Journal of Biomechanics 13: 923-927

Winter DA (1989) Biomechanics of Normal and Pathological Gait - Implications for Understanding Human Locomotor Control. Journal of Motor Behavior 21: 337-355

Yang JF, Stein RB, James KB (1991) Contribution of peripheral afferents to the activation of the soleus muscle during walking in humans. Experimental Brain Research 87: 679-687

Zatsiorsky VM (2002) Kinetics of Human Motion. Human Kinetics, Champaign, IL

Chapter VI

Conclusion

Accomplishments

In this dissertation, I used powered ankle exoskeletons to study the interaction among robotic assistance, human biomechanics, and the neural control. The purposes were to understand the general principles governing locomotor adaptation to robotic assistance. The exoskeleton assistance was proportionally controlled by the user's own muscle electromyography (EMG) signal (tibialis anterior or soleus) to provide synergistic mechanical torque. I addressed the following questions:

How do neurologically intact subjects adapt their walking patterns to a powered exoskeleton that provides dorsiflexion assistance?

My results (Chapter II) showed that subjects walked with increased ankle dorsiflexion by 9 degrees but showed different adaptation responses of the two tibialis anterior EMG bursts. The first EMG burst around heel strike (eccentric phase of tibialis anterior activation) had ~28% lower amplitudes, but the second EMG burst during swing (concentric phase) had similar amplitudes. Compared to the previous study on motor adaptation to plantar flexion assistance (Gordon and

Ferris 2007), the results suggest that dorsiflexors do not adapt to powered assistance in the same way as plantar flexors.

Do subjects walk with joint kinetics during powered walking similar to joint kinetics during unpowered walking?

The powered exoskeleton provided substantial plantar flexion assistance, ~47% of the total ankle joint moment at push-off during the powered condition. My results (Chapter III) showed that, after two sessions of practice, subjects reduced their soleus EMG activation by ~36% and walked with total ankle moment patterns similar to their unassisted gait (r^2 = 0.98±0.02). They had substantially different ankle kinematic patterns compared to their unassisted gait (r^2 = 0.79±0.12). In addition, subjects had significantly greater variability in ankle joint angle profile during powered than during unpowered walking. However, the variability in ankle joint moment profiles was similar during powered versus unpowered walking. These findings strongly suggest that humans aim for joint moment patterns with robotic assistance that are similar to joint moment patterns without robotic assistance.

Is adaptation rate dependent on the exoskeleton strength?

My results (Chapter III) showed that only half of the subjects reached steady state muscle activation patterns after two 30-minute training sessions of walking with a double-muscle exoskeleton which had greater mechanical capability. In the study of single-muscle exoskeletons, all subjects reached

steady state within the two training sessions (Cain et al. 2007; Gordon and Ferris 2007; Kinnaird and Ferris 2009). This finding indicates that greater robotic assistance provided during initial use results in a longer adaptation process than lesser robotic assistance. The increased joint impedance during initial powered walking may slow down the adaptation process.

Do subjects reduce reflex activation as a mechanism for reducing soleus recruitment with the exoskeleton?

Subjects reduced ~36% of soleus EMG when walking with the soleus-controlled plantar flexion assistance. My results (chapter IV) showed that subjects had similar H-reflex amplitude in proportion to the background soleus EMG during powered walking versus unpowered walking (p>0.05) after two 30-minute training sessions. This finding suggests that the nervous system does not inhibit the soleus stretch reflex in response to short term adaptation to the exoskeleton assistance. The nervous system might have different control strategy during long term adaptation to the exoskeleton assistance.

Do reflex responses during unexpected gait perturbations appropriately meet the mechanical requirements of gait?

I introduced a gait perturbation by turning off the robotic assistance unexpectedly at mid-stance when subjects were walking with powered assistance. My results (chapter V) showed that subjects reacted to the unexpected decrease in exoskeleton assistance by greatly increasing soleus

muscle activity about 60 milliseconds after the ankle angle deviated from the control condition. The total ankle moment (i.e., biological ankle moment plus exoskeleton assistance) was almost identical for the two conditions. The ratio of soleus H-reflex amplitude to the background electromyography was not significantly different between the two conditions. These findings demonstrated that plantar flexor responses during perturbed walking are well modulated to maintain a consistent ankle joint moment pattern.

From a basic science standpoint, these results provide insights into fundamental principles governing human locomotor adaptation. The findings suggest that humans primarily maintain similar joint moment patterns during robotic-assisted walking and when encountering gait perturbations.

From an applied science standpoint, these results will help guide the design of robotic gait devices and future robotic-assisted gait rehabilitation therapy, and the development of neuromusculoskeletal computer simulation of human walking.

References

Cain SM, Gordon KE, Ferris DP (2007) Locomotor adaptation to a powered ankle-foot orthosis depends on control method. Journal of Neuroengineering and Rehabilitation 4

Gordon KE, Ferris DP (2007) Learning to walk with a robotic ankle exoskeleton. Journal of Biomechanics 40: 2636-2644

Kinnaird CR, Ferris DP (2009) Medial gastrocnemius myoelectric control of a robotic ankle exoskeleton for human walking. IEEE Transactions on Neural Systems and Rehabilitation Engineering 17: 31-37